EFFECT OF SINTERING ATMOSPHERE ON THE PROPERTY OF CERIA DOPED TETRAGONAL ZIRCONIA POLYCRYSTALS (Ce-TZP)

A
THESIS SUBMITTED IN PARTIAL FULFILLMENT
OF THE REQUIREMENT FOR THE DEGREE OF

MASTER OF TECHNOLOGY

in

Metallurgical and Materials Engineering

By

BHABANI SANKAR SWAIN

DEPARTMENT OF METALLURGICAL AND MATERIALS ENGINEERING
NATIONAL INSTITUTE OF TECHNOLOGY, ROURKELA
MAY 2007

EFFECT OF SINTERING ATMOSPERE ON THE PROPERTY OF CERIA DOPED TETRAGONAL ZIRCONIA POLYCRYSTALS (Ce-TZP)

A
THESIS SUBMITTED IN PARTIAL FULFILLMENT
OF THE REQUIREMENT FOR THE DEGREE OF

MASTER OF TECHNOLOGY
in
Metallurgical and Materials Engineering

By
BHABANI SANKAR SWAIN

Under the Guidance
of
Prof.Ramesh C. Behera
&
Prof.S.Bhattacharyya

DEPARTMENT OF METALLUGICAL AND MATERIALS ENGINEERING
NATIONAL INSTITUTE OF TECHNOLOGY, ROURKELA
MAY 2007

Certificate

This is to certify that the thesis entitled "**EFFECT OF SINTERING ATMOSPHERE ON THE PROPERTY OF CERIA DOPED TETRAGONAL ZIRCONIA POLYCRYSTALS (Ce-TZP)**" submitted by Sri Bhabani Sankar Swain in partial fulfillment of the requirements for the award of Master of Technology in Metallurgical and Materials Engineering with specialization in "Metallurgical and Materials Engineering" at National Institute of Technology, Rourkela (Deemed University) is an authentic work carried out by him under our supervision and guidance.

To the best of our knowledge, the matter embodied in the thesis has not been submitted to any other University/Institute for the award any Degree or Diploma.

Supervisor
Prof. Ramesh C. Behera
Date Department of Metallurgical and Materials Engg
National Institute of Technology
Rourkela

Co Supervisor
Prof. S. Bhattacharyya
Date Department of Ceramic Engg.
. National Institute of Technology
Rourkela

Acknowledgement

I take this opportunity to express my deep regards and sincere gratitude for this valuable, expert guidance rendered to me by guide **Dr. Ramesh C. Behera** ,Professor, Department of Metallurgical and Materials Engineering and **Dr. S. Bhattacharyya** Professor, Department of Ceramic Engineering National Institute of Technology,Rourkela. I consider me fortunate to have had opportunity to work under his guidance and enrich myself from his vast knowledge and analysis power. They will always be constant source of inspiration for me.

My sincere thanks are to Dr G.S. Agrawal, Professor and Head metallurgical and Materials Engineering Department for his talented advice and providing necessary facility for my work.

I would also take this opportunity to express my gratitude and sincere thanks to my honorable teachers Prof. A.K.Panda, Prof.B.B.Berma, Prof U.K.Mohanty Dr.M.Kumar and Prof B.C.Ray for their invaluable advice, constant help, encouragement, inspiration and blessings.

I am also thankful toward all the professors of Metallurgical and Materials Engineering Department for helping in my works. I am thankful to Mr.Raghunath P. Rana and Mr.Yugajyoti Nayak, Research scholar of ceramic engineering department without his support this work would not have been possible.

I would also express my sincere thanks to lab. members of Department of Metallurgical and Materials Engineering, N.I.T., Rourkela, especially U.K. Sahu, R. Pattanaik,Mr. Sameer for constant practical assistance and help whenever required.

BHABANI SANKAR SWAIN

CONTENTS

Abstract

Ceria stabilized zirconia polycrystals (Ce-TZP) were prepared by varying concentration of ceria (10 and 12 mol %) by precipitation technique. The thermal analysis of the both powder show that crystallization starts at 450°C, however the total weight loss varies due to the variation of physically bonded water. The calcined powder (up to 950°C) did not show any difference in phases between 10 and 12 mol% Ce-TZP. The agglomerate size distribution of the both powder (850°C) shows monomodal distributions with D_{50}=19.83μm (10 mol% Ce-TZP) and D_{50}=5.84μm (12 mol% Ce-TZP) respectively. The non isothermal densification behavior shows the shrinkage starts at ~ 900°C for the Ce-TZP compacts. The relative density increases with increase in sintering temperature for air as well as nitrogen atmosphere. The t-ZrO_2 phase retention decreases with increasing in sintering temperature i.e. 100 vol% and 87 vol% t-ZrO_2 at 1400°C and 1600°C respectively for 12Ce-TZP respectively. Samples sintered in N_2 atmosphere shows lower relative density as well as lower fraction of tetragonal phase as compared to air sintered at all the temperatures studied. Flexural strength, compressive strength, fracture toughness and hardness were measured. A maximum fracture toughness 13 $MPa.m^{-1/2}$ was observed for 12 mol % Ce-TZP sintered in air atmosphere at 1600°C

List of Figures

List of Tables

Chapter 1

INTRODUCTION

1.1 THE IMPORTANCE OF ZrO_2 AS STRUCTURAL MATERIAL.

Zirconia is an important refractory material (M.P-2680^{0}C). It offers chemical and corrosion inertness to temperature well above the melting point of alumina. Zirconia has many novel applications in wear resistance and cutting devices. The Alumina-Zirconia Ceramics have superior strength, toughness and wear resistance when compared to conventional alumina and consequently the composite has found use a tool. Many cutting tools application have been found, item such as scissor and shear have proved particularly successful for the cutting of difficult materials such as Kevlar, out lasting conventional tool steel due to their high corrosion resistance. Seals in valves, used in chemical, slurry pumps, are also being made of zirconia ceramics components. The applications are listed below.

1. Knives and Scissors:

A major problem with metal knives and scissors when faced with tough materials such as Kevlar or when cutting large quantities of paper (which often contain dispersed minerals) is the abrasion or blunting of the cutting edge. Zirconia materials in this application retain their edge and stay sharp longer.

The key properties which make zirconia a suitable material for this application are:

1. High strength and fracture toughness coupled with high hardness (harder than the materials being cut)
2. Fine grain size so that a microscopically sharp edge may be achieved
3. The effect of transformation toughening at the machined edge of the blade which enhances toughening.

Other similar applications include blades for cutting of plastic film, magnetic tape and other tough or abrasive materials. Zirconia is also used as composite cutting tools and abrasive wheels.

2. Seals, Valves and Pump Impellers:

The handling and transport of slurries and aggressive chemicals present a difficult materials problem. High temperatures and high pressure flow lead to highly reactive and abrasive conditions. The key properties which make zirconia a suitable material for this application are:

1. Chemical resistance
2. High hardness resulting in wear resistance
3. Good surface finish to resist fouling and to minimize friction on sliding surface
4. High toughness to prevent damage during assembly or by impact in operation.

3. Orthopedics implants:

Zirconia is used as a femoral head component in hip implants. High strength and high toughness allow the hip joint to be made smaller which allows a greater degree of articulation. The ability to be polished to a high surface finish also allows a low friction joint to be manufactured for articulating joints such as the hip. The chemical inertness of the material to the physiological environment reduces the risk of infection. For this reason, only the zirconia which is manufactured from low radioactivity materials can be used in this application.

4. Refractory Applications:

Zirconia monoclinic, partially stabilized as well as fully stabilized powder is used in refractory compositions to enhance thermal shock resistance, abrasion resistance and slag resistance. These materials are used in application area such as involving such as sliding gate plates for pouring steel, and in steel immersion applications such as stopper rods and as components in submerged entry nozzles as extrusion dies for copper and aluminium wire application.

1.2. STRUCTURE:

Zirconia exhibit three well defined polymorphous, monoclinic tetragonal and cubic. It has been found that a high pressure orthorhombic form also exists. The monoclinic phase is stable up to about 1170^0C where it transform to tetragonal phase, which is stable up to 2370^0C where the cubic phase exists up to the melting point of 2680^0C.Crystallographic data are given in the following table below.

Table 1.1 Lattice parameter of Zirconia[2].

Crystal Structure	Monoclinic	Tetragonal	Cubic
Structure	a=5.156A b=5.191A c=50304 $\beta=98.9^0$	a=b=5.094A c=5.177A	a=b=c=5.124
Density	5830Kgm^{-3}	6100Kgm^{-3}	6090Kgm^{-3}

N.B: The lattice constants will vary with the type of anion and its concentration.

1.2.1. Monoclinic ZrO_2.

A precise crystal structure analysis of monoclinic ZrO_2 reveals that Zr^{4+} ions are in four fold coordination (O_{11}) on one side and on the other side by oxygen ions in triangular co-ordination (O_1). A some what idealized representation of the co-ordination polyhedron is given below Fig1and 2.

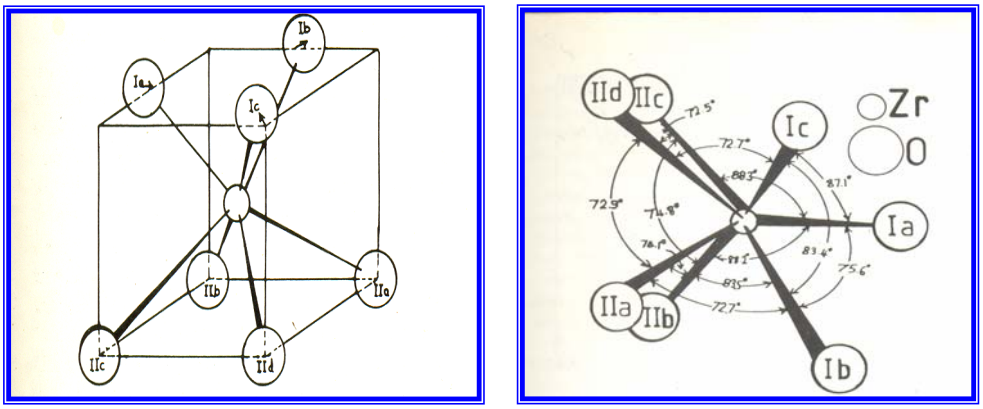

Fig. 1.1: (a)The orientation of oxygen ions together with angle of the ZrO_2 seven fold co ordination about the Zr^{+4} (b)Monoclinic zirconia [2]

1.2.2. Tetragonal ZrO_2

In its tetragonal from the Zr^{+4} enjoys eight fold co-ordinations. Four of the oxygen ions are at distance of 2.065 Å in the form of a flattened tetrahedron and four other are at 2.455 Å in an elongated tetrahedron rotated through 90^0 shown in Fig.1.2.

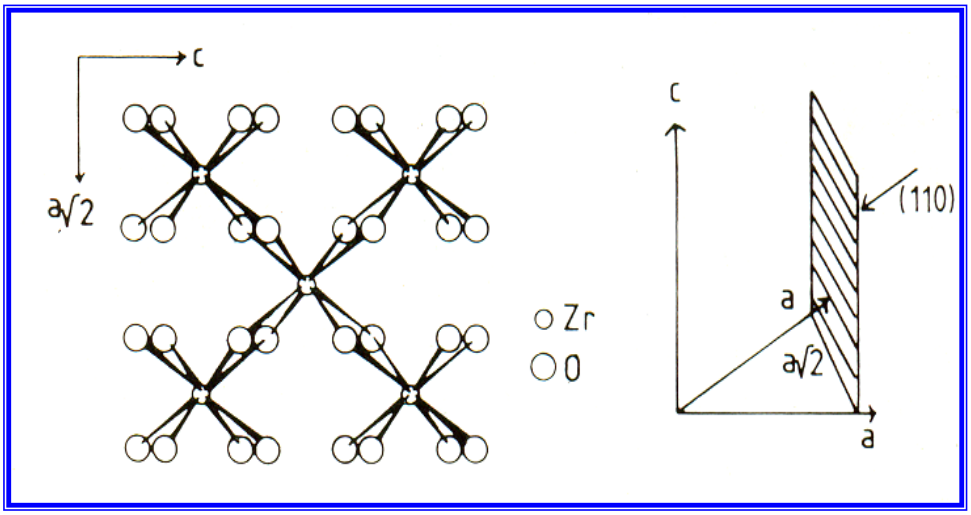

Fig 1.2: Tetragonal Zirconia [2]

1.2.3. Cubic ZrO_2

The high temperature cubic phase has a centered CaF_2 structure with each Zr^{+4} ions having eight fold symmetry with oxygen ions which are rearranged into two equal tetrahedral shown in Figure 4.

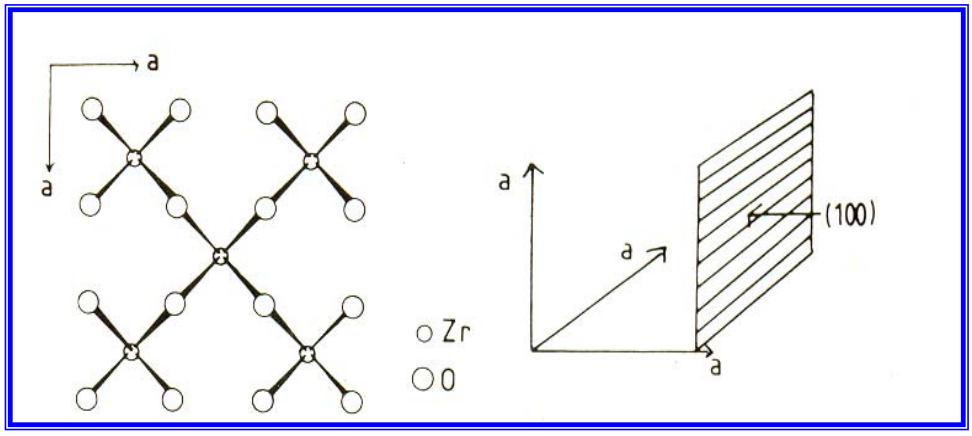

Fig 1.3: Cubic Zirconia [2]

1.3 STABILIZATION

The stabilized zirconia finds wide spread applications as a refractory material due to its high melting point and chemical inertness. Zirconia is stabilized in the fluorite type cubic phase by alloying with an appropriate amount of divalent or trivalent oxides of cubic symmetry such as MgO, CaO and Y_2O_3. This therefore, avoids the deleterious volume expansion which takes place during tetragonal to monoclinic phase change during cooling. The oxides of rare earth element have been need for stabilizer because the ions of earth element have high solid solubility, low vapour pressure and mass market application. If insufficient stabilizing oxide is added then a partially stabilizing zirconia is produced rather than fully stabilized form PSZ → (cubic solid solution + tetragonal phase) during transformation of tetragonal to monoclinic on cooling.

According to recent studies [3], in many of the stabilized zirconia system such asZrO_2–MgO, ZrO_2–Y_2O_3 & ZrO_2–CaO, the cubic phase is not an equilibrium phase and it has a tendency to change to more stable phase as the temperature reduced below the eutectoid decomposition temperature. However the rate of decomposition to an equilibrium phase is controlled by diffusion of cations whose velocity is million times slower than of oxygen ions. As a consequence, the cubic phase remains metastable at temperatures sufficiently below the decomposition temperatures.

Metal oxide-zirconia systems are a potential class of materials for use as structural materials at temperatures above 1900 K. These materials must have no destructive phase

changes. Both alkaline earth oxide (MgO, CaO,)-zirconia and some rare earth oxide (Y_2O_3, Sc_2O_3, La_2O_3, CeO_2, Sm_2O_3, Gd_2O_3, Yb_2O_3, DY_2O_3, Ho_2O_3, and Er_2O_3) zirconia systems has been examined and it has been observed that they stabilize the high temperature fluorite phase of ZrO_2 at room temperature.

A. Partially stabilized Zirconia (PSZ)

Partially Stabilized Zirconia is a mixture of zirconia polymorphs. A smaller addition of stabilizer generally-8mol% (2.7wt %) of MgO, 8mol% (3.21 wt %) of CaO or, 3-4 mol% (5.4 – 7.1wt %) of Y_2O_3 to the pure zirconia will give its structure into tetragonal phase at a temperature higher than 1000^0C, and monoclinic (or tetragonal) phase at lower temperature. Therefore PSZ is also called as Tetragonal Zirconia Polycrystal (TZP).PSZ is a transformation toughened material. It (PSZ) has been used where extremely high temperatures are required. It is used as refractory because it has low thermal conductivity ensure low heat losses and the high melting point. Zirconia is not wetted by many metals and is therefore an excellent crucible material when slag is absent. It is also used experimentally as heat engine components, such as cylinder liner, piston caps and valve seats.

B. Fully stabilized zirconia

Generally, addition of more than 16 mol % (7.9 wt %) CaO, 16 mol % (5.06 wt %) MgO and 8 mol %(13.75 wt %) Y_2O_3 into zirconia structures is needed to form a fully stabilized zirconia. Its structure becomes cubic solid solution, which has no phase transformation from room temp up to 2500^0C. As good ceramic ion conducting materials, fully yitria stabilized zirconia (YSZ) has been used in oxygen sensor and solid oxide fuel cell (SOFC) applications. The SOFC applications have recently been attracting more world wide attention due to their high energy transfer efficient and eco friendly ness.

Binary Phase Equilibria

Phase equilibria of zirconia with other oxide systems are:

a. ZrO_2 - MgO System
b. ZrO_2-Y_2O_3 System
c. ZrO_2-CaO System
d. ZrO_2-CeO_2 System

These systems have fundamental to the application of zirconia as an engineering ceramic both at low temperature where a second oxide phase addition can change the property via the

microstructures change. At high temp where a second cation can induce dynamic changes of microstructure and thus the properties

1.3.2. ZrO2–MgO System:

This system has been investigated by several researchers and the resulting phase diagrams differing considerably. An investigation using well crystallized pure oxide reagents and x-ray diffraction lattice parameter measurements has produced an equilibrium diagram. Fig 1.4 shows one such giving reasonable agreement with independent data, namely the electrical conductivity dependence of magnesium oxide solubility in monoclinic and tetragonal zirconia.

According to the Fig.1.4, there is little or no solubility of MgO in monoclinic zirconia up to the tetragonal transformation temperature. The solubility of MgO in the tetragonal zirconia increases slowly with temperature, but is still less than 1% at 1300^0C. A cubic solid solution becomes stable above 1400^0C with a eutectoid composition at 13 mol% MgO. A homogeneous fluorite structure solid solution then exists at this composition above 1400^0C, the composition range increasing considerably with temperature.

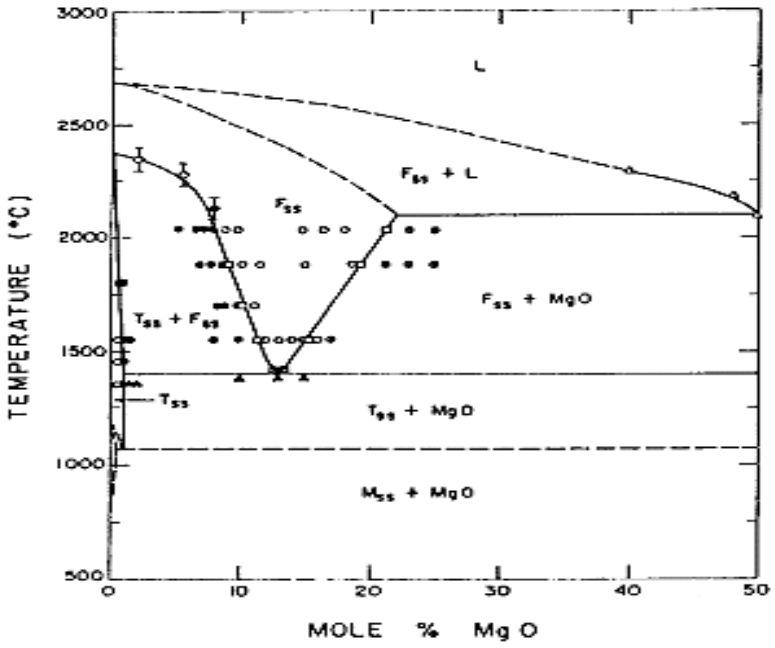

Fig 1.4: ZrO_2-MgO phase diagram [4]

A feature of technological importance is the cubic s.s and tetragonal s.s phase field. On heating in the totally cubic s.s field for compositions in the range 6-8.5 mol% MgO, a homogeneous solid solution results. If this material is now quenched into the cubic s.s + tetragonal s.s phase field, lenses or oblate spheroids of tetragonal s.s nucleate and grow. On quenching to room temperature, depending on size, the tetragonal s.s lenses can have the ability to transform to monoclinic zirconia, a process which results in a volume change and affects the mechanical properties considerably. This process is fundamental to the application of the partially stabilized zirconia (PSZ's). Another significant and well established feature of the ZrO_2 –MgO system is the decomposition of the cubic solid solution into the constituent oxide below 1400^0C and again below 1240^0C. As this occurs, the MgO has a tendency to precipitate along grain boundaries and at intergranular voids. This was believed to degrade the mechanical properties of the ceramic, making it unsuitable for application in the temperature range 1000^0-1400^0C. More recent work contradicts this belief; prolonge ageing at 1100^0C for a 6.8-7.9 mol % composition gave no such decomposition and developed a strong and thermally shock resistant ceramic. This heat treatment caused the formation of $Mg_2Zr_5O_{12}$, a metastable intermediate ordered compound referred to as α phase. A β-$Mg_2Zr_5O_{12}$ ordered structure with rhombohedral symmetry has also been reported which is considered to be a non equilibrium phase found in the decomposed cubic regions between the tetragonal precipitates. The formation of such complex phases by the use of sub eutectoid ageing is now used commercially to increase the mechanical and thermal shock properties of MgPSZ.

1.3.2. ZrO_2 – CaO System:

Calcium oxide is one of the most common of the oxides used to form a solid solution with ZrO_2. The most recent phase diagram Fig. 1.5, shows a more extensive fluorite phase field at 2000^0C than reported earlier. This cubic phase which was considered to be stable down to room temperature is now known to undergo a decomposition reaction below ~ 1220^0C.

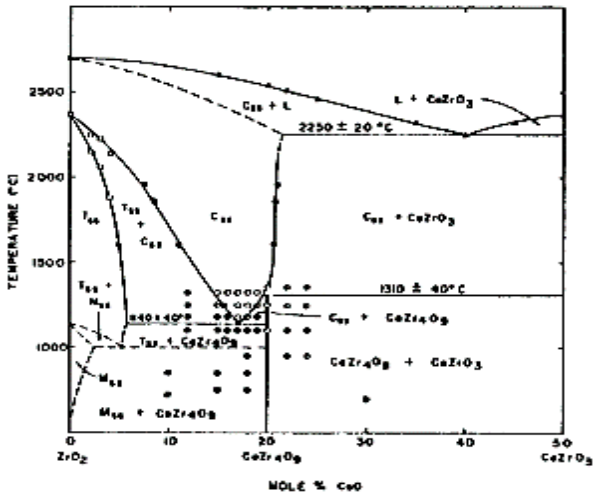

Fig 1.5: Phase diagram for ZrO2-CaO [5]

There are three main regions of interest. Up to ~ 6 mol % CaO and below 2000^0C tetragonal s.s. is stable which when cooled passes into a two phase region of tetragonal s.s. + monoclinic s.s. Further cooling results in production of monoclinic s.s + $CaZr_4O_9$. This last reaction only occurs after extended periods of time. Above 6 mol % CaO a two phase region of tetragonal s.s. + cubic s.s. exists up to ~ 17 mol % CaO above 1140^0C Within this phase field the materials are known as partially stabilized zirconia (PSZ).

On rapid cooling the tetragonal s.s. will transform to monoclinic s.s. in a metastable matrix of cubic s.s Slow cooling below 1140^0C but above 1000^0C results in a tetragonal s.s. phase, together with the decomposition product of the eutectoid reaction. Further cooling below 1000^0C causes the martensitic transformation of the tetragonal s.s. to monoclinic s.s. Similar reaction takes place from compositions within the cubic phase field, compositions in this range being known as fully stabilized zirconia. They are in fact metastable, but the slowness of the reactions at the temperatures which are usually encountered in devices allows the properties of the defect cubic structure to be utilized, although after extended periods of time at > 800^0C 'ageing' occurs, generating micro structural changes in the material. A detailed account of the precipitation phenomenon has been given by Marder et al [6].

1.3.3. ZrO2-Y_2O_3 System:

The most important feature of the ZrO_2 - Y_2O_3, phase diagram is the decrease in temperature of the tetragonal monoclinic transformation with increase in Yttria content, a phenomenon which does not occur with MgO and CaO additions. It would be noted that HfO_2 additions increase the transformation temperature. This behavior has important implications for both the design and use of toughened ceramics produced as either partially stabilized zirconia or as heterogeneous two phase systems, since the upper temperature limit for any application is determined by the monoclinic tetragonal transformation temperature.

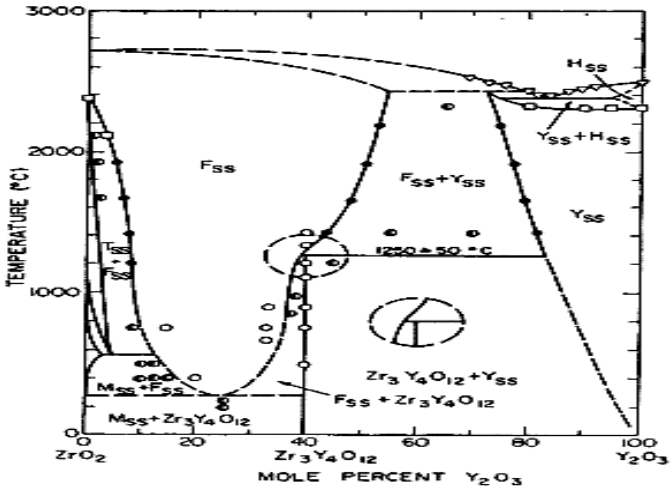

Figure 1.6: Phase diagram for ZrO_2-Y_2O_3 [6]

With increase in temperature, above the monoclinic phase field, a narrow monoclinic + tetragonal field is encountered before a transformable tetragonal field is reached. The transformable tetragonal solid solution, i.e., a phase that will transform on cooling to the monoclinic structure, exists in composition range 0-5 mol % $YO_{1.5}$.For compositions containing greater amounts of yttria a mixture of non transformable tetragonal and cubic solid solution exists, Finally increasing the yttria content further results in a homogeneous cubic solid solution, stable from room temperature to the melting point. The nature and composition of the tetragonal, the non transformable tetragonal (t') and the transformation of these phases from the cubic have been discussed in detail by Anderson et al [7].

The slope of the dividing the transformable tetragonal phase field and the tetragonal plus cubic (T + F in fig 1.6) is of significance. By sintering a fixed composition material at increasing temperatures in the range 1300-1650^{0}C, the amount of cubic phase will increase with sintering temperature. Furthermore should a structure be required which contains

100% tetragonal, i.e., no cubic phase present, then for any temperature there is only one composition which changes with temperature. Generally the tetragonal zirconia ceramics fabricated in this alloy system are 'overstabilised' for several reasons, not withstanding the development of properties which are below the maximum attainable.

The 3 mol % Y_2O_3 ceramic provides insurance against under stabilization due to chemical homogeneity, when spontaneous transformation to the monoclinic form would lead to degradation in mechanical properties. The over stabilization also allows a larger critical particle size to remain meatstable when 'constraint' is removed by heating in a water containing atmosphere at ~ 200^0C. The sensistivity of the material to high temperature aqueous environments is a cause for concern and has led to the development of the ZrO_2–CeO_2 alloy system.

1.3.4. ZrO_2-CeO_2 SYSTEM:

There is currently interest in the partially stabilized zirconia of this system. However, as shown in the phase diagram (Figure 8), there is not a fully stabilized composition down to low temperatures for this system. The catastrophic monoclinic to tetragonal phase transformation limits this material's use as a high temperature structural material.

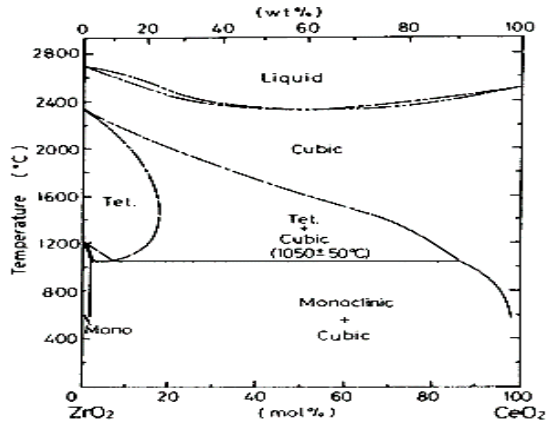

Fig.1.7: Phase diagram for ZrO2-CeO_2 [8]

The vapor pressure of ZrO and Zr is actually higher than their vapor pressure above pure ZrO_2.This is an interesting consequence of vaporization of Ce_2O_2 as CeO_2(g) and CeO(g). In the solid solution, $Ce_2O_{3.2}$(ZrO_2), when both these species are formed, very little O(g) is generated. In fact, since the species are not formed in equal amounts, some oxygen must come from ZrO_2. There is no suppression of the vaporization decomposition processes and the vapor pressures of ZrO and Zr go up. These vapor pressures are not simply related to the activity of ZrO_2, which must remain one or less in solution.

1.4. TRANSFORMATION TOUGHENING MECHANISM

It is generally recognized that apart from crack deflection which can occur in two phase ceramics, the tetragonal to monoclinic transformation can develop significantly improved properties via two mechanisms.

i. Micro cracking

ii. Stress induced transformation toughening.

1.4.1. MICRO CRACKING

This can be induced by the incorporation of ZrO_2 particles in a ceramic matrix such as Al_2O_3.On cooling through the transformation temperature (t-m), the volume expansion of 3-5% occurring in the ZrO_2 particles causes a crack to form as shown in Fig. 1.8 (a,b).Tensile stresses are generated around the transformed particle which induces micro cracks in the matrix. These by ability to extend in the stress field of the propagating crack or to deflect the propagating crack can absorb or dissipate the energy of the crack, there by increasing in toughness of the ceramics. The optimum conditions are met when the particles are large enough to transform but only small enough to cause limited micro crack development.

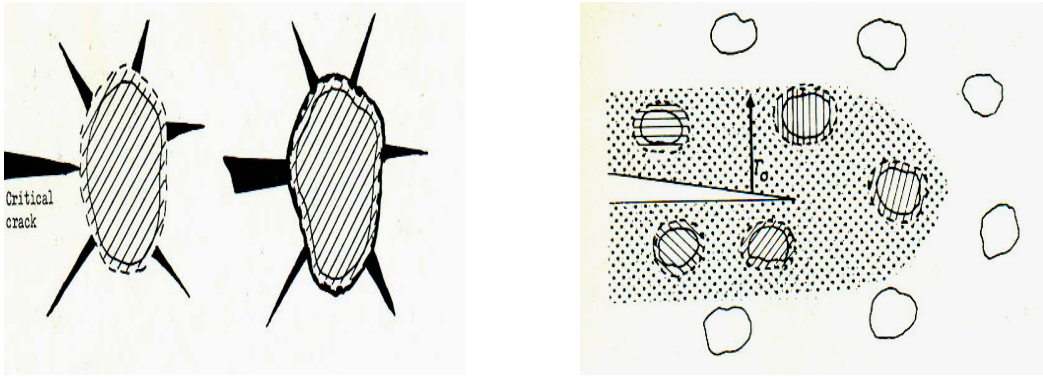

Figure 1.8 (a) Stress induced transformation of metastable ZrO_2 particle in the elastic stress field. (**b**)The crack propagating in to the particle is deviated and become bifurcated.

1.4.2. STRESS INDUCED TRANSFORMATION TOUGHENING

We know that at much higher temperature, the zirconia changes from tetragonal to cubic structure. With proper chemical additions and heat treatments, a micro structure can be achieved during cooling that consists of 'lens shaped' precipitates of tetragonal zirconia in cubic grains of zirconia as shown in Fig. 1.8 (a).Normally the tetragonal material would transform to the monoclinic form during cooling with volume expansion (3-5%) and shear

strain (1-7%) but the matrix constraint of the surrounding cubic zirconia prevents this expansion, so the tetragonal form is retained all the way down to room temp. as a result each tetragonal zirconia precipitate is under stress and full of energy that it wants to be released. If a crack is made to extend under stress, which is shown in fig 1.8 (b), then a large tensile stresses are generated around the crack, especially ahead of the crack tip. These stresses release the matrix constraint on the tetragonal zirconia particles and therefore will allow transforming the tetragonal zirconia into monoclinic symmetry. Therefore the volume expansion (3-5%) and shear strain (1-7%) with the martensitic reaction. The associated of t-m transformation of t-ZrO_2 generate compressive strain, which stp the crack propagation through the ceramic and thus increase in toughness and strength.

Chapter 2

LITERATURE REVIEW

LITERATURE SURVEY:

Ceria stabilized tetragonal zirconia polycrystalline ceramics possess distinct advantages over other conventional structural ceramic materials (Garvie et al 1975; Evans and Cannon 1986) because of their better thermal stability in moist environments (Matsumato 1978), wider range of solid solubility in tetragonal region and coefficient of thermal expansion matching with that of iron alloys (Tsukuma and Shimada 1985; Nettleship and Stevens 1987). Consequently, ceria stabilized zirconia ceramics have been investigated extensively for structural applications.

The highly improved mechanical properties in these transformation toughened ceramics are related to the stress induced transformation of the metastable tetragonal grains to the monoclinic phase at the crack tips (McMeeking and Evans 1982; Chen and Reyes-Morel 1986; Hannink et al 2000). Therefore, the transformability of the metastable tetragonal phase in the process zone plays a dominant role in the ultimate attainable mechanical properties of these materials. The grain size and micro-structure of these materials are difficult to control in conventional technique such as ball milling for powder preparation. The larger ball milled particles sintered at much higher temperature leading to considerable grain growth, which did not permit retention of desired tetragonal phase and high values of mechanical properties in the material (Wang et al 1992). Most of the earlier studies on CeO_2 –ZrO_2 system were with powders prepared by conventional methods and the results are inconsistent due to the poor homogeneity and sinterability of the powders (Wang et al 1992). Recently few attempts have been made to prepare CeO_2–ZrO_2 using chemical methods and only a limited effort has been made to understand the effect of CeO_2 content and grain size on the mechanical properties of the system (Wang et al 1992; Maschio et al 1992). Various additives and sintering aids have also been tried to improve sintered density and flexural strength of the material (Maschio et al 1998; Kojima et al 2000).

Recently high purity, chemically homogenous and reactive ceria stabilized zirconia powders have been prepared by chemical methods (Yin et al 1999; Matsui and Ohgai 1999) and sintered ceramics having considerably high density and transformable tetragonal phase have been obtained using these powders. However, little effort has been made to establish structure–property correlation in the sintered ceramics (Yoshioka et al 1992).

Todokoro et.al [9] prepared Ultrafine zirconia–12 mol% ceria powders by the co-precipitation technique. The azeotropic distillation with n-butanol was carried out by them to ensure complete elimination of the residual water in the precipitate. This procedure has proved to be quite effective in preventing the formation of agglomerates, which are

responsible for in homogeneities in the sintered microstructure, and for non-densification at low temperatures. They found that, the crystallization of the solid solution occurs at 430^0 C as determined by thermal analyses. The specific surface of the calcined powder is 127.9 m^2/g and the pore size distribution exhibits only a maximum at approximately 9 nm. Total shrinkage of the compacted powder reached 30% at 1200^0 C. Specimens with apparent densities >95% of the theoretical density and average grain size of 230–400 nm were obtained after sintering at 1200 ^{0}C.They conclude that, The use of azeotropic distillation for gel dehydration greatly improves the physical properties of the solid solution. This powder allowed for preparing ceramic specimens with relative densities >95%, average grain sizes <300 nm, and total stabilization of the tetragonal phase at a sintering temperature as low as 1200 ^{0}C.

J. Vleugels et al [10] found that Controlled annealing of fully dense air-sintered Ce-TZP ceramics in Ar (5% N_2, 1.2 ppm O_2) allows improving the surface toughness from 8 to 16$MPam^{1/2}$. Optimum mechanical properties were obtained after 10–20 min annealing at 1450 ^{0}C. The increased toughness was explained in terms of the reduction and segregation of cerium, resulting in a t-ZrO_2 matrix with enhanced transformability due to reduced stabilizer content and the change in grain morphology. They explained that during annealing, the Ce^{+4} ions dissolved the tetragonal ZrO_2 lattices are partially reduced to Ce^{+3}. Controlled annealing of fully dense air-sintered Ce-TZP ceramics in Ar (5% N_2, 1.2 ppm O_2) allows to improve the surface toughness from 8 up to 16$MPam^{1/2}$ .Optimum mechanical properties were obtained after 10–20 min annealing at 1450°C. The increased toughness was explained in terms of the reduction and segregation of cerium, resulting in a t-ZrO_2 matrix with enhanced transformability due to reduced stabilizer content and the change in grain morphology.

Ceria stabilized zirconia powders with ceria concentration varying from 6 to 16 mol% were synthesized using spray drying technique by Sharma et.al [9] Powders were characterized for their particle size distribution and specific surface area. The dense sintered ceramics fabricated using these powders were characterized for their microstructure, crystallite size and phase composition. The flexural strength, fracture toughness and micro hardness of sintered ceramics were measured by them. High fracture toughness and flexural strength were obtained for sintered bodies with 12 mol% of CeO_2.They found that Flexural strength and fracture toughness were dependent on CeO_2 concentration, crystallite size and phase composition of sintered bodies. Correlation of data has indicated that the sintered density, proportions. The transformable tetragonal phase was the key factor in controlling the fracture toughness and strength of ceramics. It was observed that the spray drying synthesis

method is effective to prepare nano-crystalline tetragonal ceria stabilized zirconia powders with improved mechanical properties. The sintered density of ceramics was > 98.2% except for 6Ce–ZrO_2. The lower density is due to the higher monoclinic phase leading to development of micro cracks during sintering. It was observed that the powders containing 6 and 8 mol% CeO_2 contained m + t phases, powders having 10, 12 and 14 mol% CeO_2 were fully tetragonal whereas 16 mol% CeO_2 addition gives rise to cubic phase. The axial ratio (c/a) decreased with increasing in CeO_2 concentration from 6 to 16mol%.The amount of metastable transformable tetragonal (t) phase decreases and non-transformable tetragonal (t') phase increases with increase in ceria concentration above 12 mol%. Powders synthesized from polymer precursor. They observed that crystallite size of zirconia ceramics decreases with increase in ceria concentration and flexural strength and fracture toughness increase sharply with increase in ceria concentration up to 12 mol% and start decreasing slowly with further increase in ceria concentration. This may be attributed to increase in transformable tetragonal phase in the material up to 12 mol% CeO_2 Concentration and thereafter decrease in transformable tetragonal phase and increase in non transformable tetragonal phase with further increase in ceria concentration. They reported that the variation of ceria content in zirconia has very little effect on the hardness of Ce–ZrO_2. They found that the hardness of 6Ce–ZrO_2 was also slightly lower due to its lower density and micro cracks. The average grain size was about 2 μm. The lower grain size and high density of ceramics in the present studies may be attributed to fine starting powders and lower sintering temperature. The finer grains have vital role in achieving higher flexural strength in the present study. Also investigated the effect of addition of 20 wt% alumina in 12Ce–TZP gives the much improved strength (1200 MPa) with moderate toughness (9.2 $MPam^{1/2}$) as compared to earlier study (Cutler et al 1991).

Matsuzawa et.al. [11] investigated non-elastic strain behavior in detail for several different zirconia ceramics (Y-TZP, Y-FSZ, Mg-PSZ and Ce-TZP), and a possible mechanism for anelasticity was discussed by them . Y_2O_3 -doped zirconia ceramics (Y-TZP and Y-FSZ) exhibited a remarkable degree of anelastic strain, as does Mg-PSZ to a lesser extent. On the other hand, Ce-TZP hardly produced anelastic strain. They suggest that the anelastic properties depend on the particular dopant additive, irrespective of the crystallographic phase. In Mg-PSZ, besides the anelastic strain, a time-dependent non-recoverable strain is produced under loading. They reported that this non-recoverable strain corresponds to the strain caused by a phase transformation and suggested that the anelastic

properties could be significantly influenced by the level of oxygen vacancy in the matrix, and that the anelastic strain might be produced by a slight shift of ionic species.

Four types of zirconia ceramic, Ce-TZP, 3Y-TZP, 8Y-FSZ and Mg-PSZ, were heated at 1000^0 C in hydrogen gas. The various mechanical properties before and after the heat treatment for reduction were investigated by Matsuzawa et.al [12].

They proposed the results as follows.

(1) Ce-TZP was very effectively reduced after the heat treatment in hydrogen but the other samples were not reduced in spite of the severe reducing condition. The drastic weight loss and the increase of internal friction were observed in the reduced Ce-TZP due to the large number of oxygen vacancies introduced into the matrix.

(2) The sufficient reduction effectively increased the hardness, but on the other hand, decreased the fracture toughness. It was found that the serious decrease of fracture toughness should be predominantly caused by low transformability at the reduced Ce-TZP. The in-corporation of hydrogen into the Ce-TZP matrix was detected after the heat treatment in hydrogen. However hydrogen-induced embrittlement did not occur for the Ce-TZP ceramics.

(3) The anelastic property of Ce-TZP was extremely enhanced by the increase of oxygen vacancies. It is possible that anelasticity is efficient at improving the tensile strength.

Tiefenbach et.al [11] studied on the t-m and m-t transformations in Ce–TZP by dilatometry and impedance sp ectroscopy. They used 9 mol% CeO_2 stabilized ZrO_2 powder (9Ce–TZP, Unitec,UK) Plates of 654512 mm were produced by pressing, cold isostatic repressing and sintering at 1400^0 C for 2 h in air. In order to vary the grain size, subsequent annealing at 1400 ^{0}C in air for 16 to 256 h was carried out. The required specimen sizes were shaped from the plates by diamond cutting and grinding. All the specimens were annealed at 1200 ^{0}C for 1 h to remove residual stresses and the grinding induced monoclinic for the investigation of the transformation process in TZP ceramics.phase in the near surface region. They used dilatometry and impedance spectroscopy for their characterization. They reported that impedance spectroscopy is an useful tool

Yuan et.al [13] investigated on synthesis and characterization of CeO_2 coated ZrO_2 powder-based TZP in air atmosphere by using suspension drying method. The dried hygroscopic powder was subsequently calcined in an alumina crucible in air at 800 ^{0}C for 1h in order to obtain the Al_2O_3 doped CeO_2 coated ZrO_2 nano powder. The samples obtained were sintered in a muffle furnace in air for 1h at 1450 ^{0}C. The heating rate was 15^0C/min, cooling was performed naturally. They observed that near full densification could be achieved with Al_2O_3 doped CeO_2 coated ZrO_2 nanopowder by pressure less sintering in air at

1450^0 C. The CeO_2 dissolved completely in the ZrO_2 matrix during sintering and stabilized the t-ZrO_2 phase, resulting in Ce-TZP with excellent fracture toughness. The starting material used by them was commercial Daiichi grade CEZ12; a 12 mol % CeO_2 stabilized co-precipitated ZrO_2 powder. The powder was cold isostatically pressed into cylinders, with a diameter of 1 cm and a length of 2 cm, under a pressure of 300 MPa for 3 minutes. The samples were sintered at 1450°C for 20 minutes by means of microwave heating in argon (with the addition of 5 vol%N_2 to avoid plasma formation in the microwave cavity) and in air . The microwave-heating set-up, in which a tubular SiC susceptor was used to realize hybrid sintering, the gasses used for hybrid microwave sintering are synthetic air, nitrogen and argon. The oxygen partial pressure is estimated to be 10 Pa at the sintering temperature of 1450°C.They utilize a number of characterizations tools such as Vicker indentation method to determine the hardness and fracture toughness. Phase composition and grain size were measured by XRD and SEM analysis.

Yuan summarized as follows:

(1)For the first time, they reported that 12 mol % CeO_2 stabilized ZrO_2 powders prepared by co-precipitation route can be successfully sintered to full density in 20 minutes at 1450°C in argon with 5 vol % nitrogen.

(2)A high fracture toughness of 16 $MPam^{1/2}$ was achieved in the inert atmosphere, whereas a toughness of 6 $MPam^{1/2}$ was measured for the air sintered samples. The mechanism proposed for enhanced toughness of the samples sintered in inert atmosphere is the partial reduction of Ce^{+4} concomitantly reducing the CeO_2 content in the t-ZrO_2 grains and increasing the Ms temperature.

(3)The phase composition and properties of the Ce-TZP ceramic were found to be strongly dependent on the sintering atmosphere. The Ce-TZP ceramics sintered in Ar (5 vol % N_2) contain t-ZrO_2 and a (Zr,Ce)O solid solution, whereas those sintered in air are fully tetragonal. Sintering in argon with 5 vol % nitrogen significantly increased the M temperature of the Ce-TZP while compared to sintering in air.

Hydrothermally synthesized nano-size CeO_2 powders, chemically precipitated CeO_2 powders and commercial micron-size CeO_2 powders were investigated by Zhou et.al [14] by DTA/TGA and TEM. The sintering behavior of these powders was studied by continuous monitoring of the shrinkage kinetics. The microstructural features of the sintered specimens were observed by SEM. They reported the sinterability of the CeO_2 powder compact increased with decrease in particle size.

T. Sato et al. [17] studied the Sintering behaviour of ceria-doped tetragonal zirconia powders crystallized and dried using supercritical alcohols. They describe the sintering behaviour of 12Ce-TZP powders which has been crystallized and dried using supercritical alcohols for studying the effect of crystallizing conditions on the sinterability. They achieved about 95%of theoretical density

Zirconia powders containing 12 mol% ceria have been prepared by the co precipitation technique by Attaoui et.al [16]. The aim of the present work was to obtain nanosized powders with suitable sinterability and reduced grain size in the sintered ceramic by means of this solution technique in its simplest route, that is, without using any milling or other special procedure. For comparison purposes, Attaoui et.al used specimens of the same composition have been prepared by the powder mixing technique. The optimization of some processing variables allowed for obtaining sintered specimens with apparent densities of 98% of the theoretical value, 100% of tetragonal phase, and 500 nm of average grain size.

Ceria partially stabilized zirconia ceramics (Ce-TZP) with identical grain size and different amounts of transformation toughening were processed to investigate the influence of phase transformation on static and cyclic fatigue crack growth. Static crack growth is governed by environmentally stress induced corrosion at the crack tip and it is highly influenced by the crack shielding due to the phase transformation. Three fatigue mechanisms are expected to be operative at different proportions depending on the amount of transformation: wedge effect due to debris, degradation of bridging and modification of the shielding effect of the transformation zone. However, it is difficult to separate the contribution of the different mechanisms as grain bridging is induced by crack arrest due to phase transformation.

From AFM and MEB observations of crack path, they concluded that phase transformation induces two other toughening mechanisms:

(i) Crack bridging by monoclinic transformed grains resulting from crack arrest due to the shielding effect of the transformation zone.

(ii) Crack branching operating within a large zone in the presence of autocatalytic transformation. It is thus difficult to separate the contribution of each mechanism, particularly, the influence of grain bridging and transformation first mechanism is different from the simple grain bridging due microstructure, generally observed in non transforming ceramics.

Investigations were carried out by Gogotsi et.al [17] on four tetragonal zirconia polycrystalline (TZP) ceramics of differing grain size containing 9 mol% CeO_2,. Precision

flexural tests on these materials were conducted to determine the elastic modulus, the non-linear deflection and the associated acoustic emission during such testing. The deformation was characterized in terms of the number and size of the transformation bands that developed during the non-linear response. The finest grained material initially exhibited permanent set without the presence of such bands, whereas all the coarser grained materials showed a linear relationship between the summation of the band widths and the residual deflection. The acoustic emission and plastic strain behaviour are discussed in terms of the number and size of the stress induced phase transformation bands.

Nitrogen_incorporation into pure and doped zirconia studied by S. Gutzov [21].The defect chemistry of the nitrogen incorporation into pure and cation (Y^{3+}, Eu^{3+}, Ce^{4+}, Mg^{2+}, Ca^{2+})-doped ziconia is quantitatively described using simple thermodynamic considerations, allowing the calculation of the anion vacancy concentration as a function of the nitrogen and oxygen pressure in the surrounding atmosphere. The nitridation of zirconia occurs at temperatures between 1400^0C and 2200^0C in nitrogen atmosphere leading to the formation of zirconium oxynitrides (nitrogen-containing zirconia). Theoretical and experimental investigations show that the nitridation of zirconia is to be explained as a grain-size dependent reaction, equilibrium conditions after 2h of nitridation are observed at temperatures of 1900^0C and higher. Nitrogen-containing zirconia exhibits exceptional mechanical, electrical and optical properties compared to undoped zirconia. A combination of doping in the cation and the anion sub lattice allows controlled synthesis of anion-deficient fluorite-type materials with ordered or randomly distributed anion vacancies. At ambient pressure, ZrO2 exists in three polymorphs: monoclinic (m-ZrO2), tetragonal (t-ZrO2) and cubic zirconia(c-ZrO2). The high temperature t-ZrO2 and c-ZrO2 phases are stabilized at room temperature by the presence of oxygen vacancies. In this way the nitridation is a very useful approach to prepare metastable zirconia phases and to affect their physical properties.
They were presents a quantitative physicochemical model for nitrogen incorporation into the zirconia lattice and clarifies the thermodynamics of incorporation. The nitridation of pure and cation-doped zirconia is of interest because of the promising optical properties of ZrO2: Eu, ZrO_2: Ho, ZrO_2: Sm and ZrO_2: Tb materials.

Chapter 3

EXPERIMENTAL PROCEDURE

3.1. SAMPLE PREPARATION:

3.1.1: Estimation of ZrO_2 from zirconium oxychloride and Ceria from Ammonium Ceric Nitrate

A known amount of $ZrOCl_2$ was dissolved in distilled water. The concentration of $ZrOCl_2$ was taken 0.75mole/litre. The solution was stirred and filtered to ensure complete mixing and remove any dirt or other impurity.3 ml of $ZrOCl_2$ was taken in a weighed crucible and to it excess NH_4OH was added to ensure complete precipitation of $Zr(OH)_4$.The precipitate was dried and calcined at 1100 ^{0}C for 2 hours. From the weigh difference after calcinations and the empty platinum crucible, the amount of ZrO_2 obtained per ml of $ZrOCl_2$ solution was obtained. The experiment was repeated to ensure reproducibility. The presence of ZrO_2 in the calcined powder was confirmed by phase identification through XRD. Similar method was also carried out for estimation of Cerium ammonium nitrate.

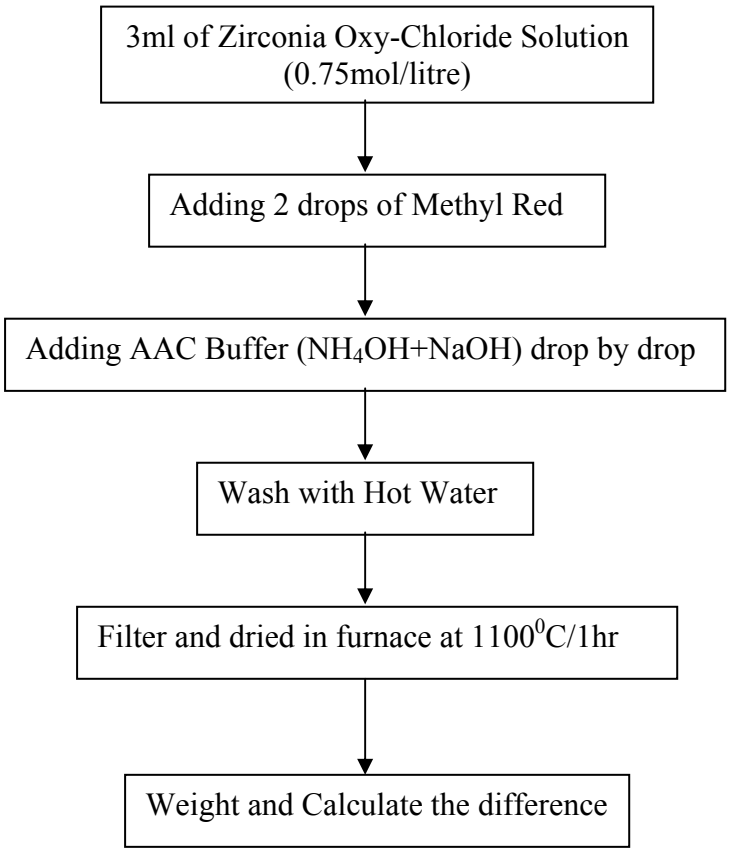

Fig. 3.1: Flow Chart of Estimation of Zirconia from Zirconia Oxy-Chloride

The same procedure was applied for estimation of Ammonium Ceric Nitrate

3.2: Powder Synthesis

Ceria stabilized zirconia powders were prepared by co-precipitation technique using 0.75mol/lit of zirconium oxychloride (AR Grade) solution and Ammonium Ceric Nitrate (AR Grade). Both the solutions were mixed and filtered if necessary. NH_4OH (1:1)solution and above solution of Zirconia oxy chloride and ammonium ceric nitrate was separately taken in two beaker .was added continuously and pH maintained 10.This was achieved by continuous adding of ammonia because continuous addition of Zirconium oxy-chloride solution and ammonium ceric nitrate lower the pH. The Precipitation was continuously stirred about half an hour. The precipitates were allowed to settle till a clear supernatant liquid was obtained. Subsequently the gel was washed with hot water in order to free it from chlorides and excess ammonia, followed by alcohol washing. The hydrated samples were oven dried and ground to fine powder.

3.3: Preparation of green Specimen

3.3.1. Binder Addition:

Binder was added to give calcined powder green strength. Here 4 wt. % PVA (Poly Vinyl Alcohol) solution was used as binder. The calcined powder was taken in a mortar and as per the weight of the powder 4wt. % PVA solution was added to it. Then it was mixed thoroughly with the help of mortar and pestle to get proper mixing. After mixing, it was dried for removal of water content of the binder solution. After that the binder added Ceria doped Zirconia powder (dried) was grinded with the help of agate-mortar to fine powdered form.

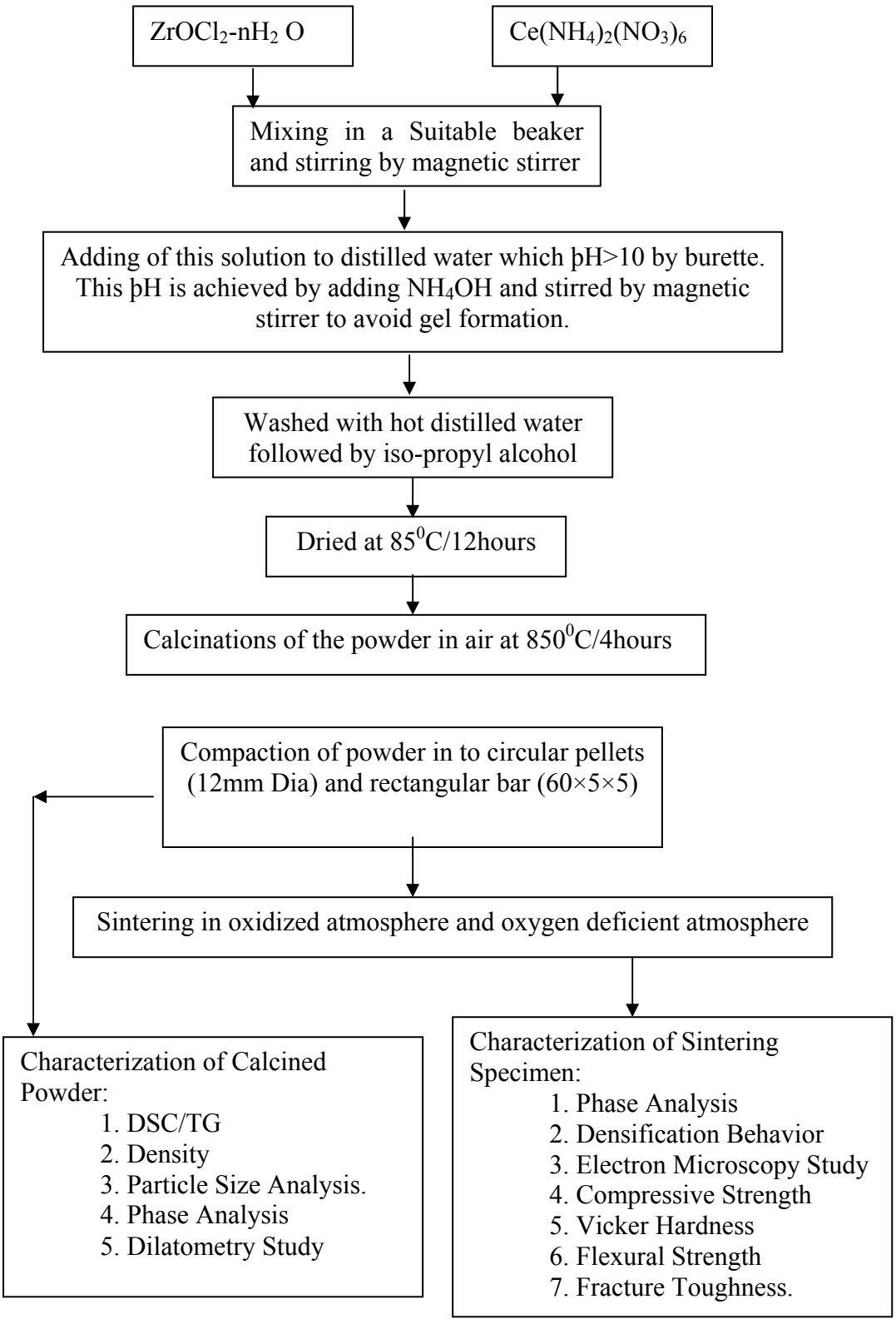

Fig. 3.2: Schematic Chart of processing of Ceria Doped Zirconia Powder and Sintering and Characterizations

3.3.2. Green Compaction:

The binder mixed powder was compacted to give a desired shape for further characterization. About 1.10 grams of PVA added calcined Ceria doped Zirconia powders were taken for making each pellet. The weighing was done in an electronic balance. The powders were pressed uniaxially in a steel die into cylindrical pellets (12 mmΦ, 3mm high). The steel die was cleaned using acetone and cotton. It was lubricated using 3wt.% Stearic acid. The powder was added slowly into the die with bottom punch. Then it was tapped slowly to allow uniform leveling of the powder and better filled density. Then the top punch was applied slowly. The pressing was done uniaxially at 270MPa in a Hydraulic Press (10 T, SoilLab Testing Instruments,India). A holding time of 60seconds was given for pressing of each sample. The pressure was released to get the green pellet. The pressure was decreased slowly to avoid pressing defects in the samples. In this manner a number of pellets were prepared. The steel die was cleaned up and lubricated after each pellet pressing.

Similarly, rectangular bars of dimensions 60mm x 5mm x 5mm were pressed in a rectangular die of the given dimensions. As mentioned the die was cleaned up with acetone and was lubricated with 3wt. % Stearic acid. To get the specified dimensions specific amount of PVA mixed fine powder was put into the die slowly. The sample was then pressed uniaxially at 270MPa. The holding time at peak load was 90seconds. The green dimension of every specimen was noted using a Slide Caliper.

3.4: Sintering

The uniaxial pressed green compacts were sintered in air as well as nitrogen atmosphere with a heating rate of 3°C/min at the temperature range 1400^0-1600^0C with a holding time of 4 hours at the peak temperature as well as sintered sample at temperature variation of 1400^0C to 1600^0C.

3.5. Characterization:

3.5.1: Particle Size Analysis

A laser diffraction method with a multiple scattering technique has been used to determine the particle size distribution of the milled powder. To measure the particle size through laser scattering method, the instrument detects the correlation between the intensity and the angle of light scattered from a particle, and then calculates the particle size based on the Mie-scattering theory. In order to capture scattered light signals over this range of angles,

the equipment utilizes a number of high-angle and back-scatter detectors, together with a short wavelength blue LED laser. As the particle size becomes smaller, the scattered light signal shifts to the side and rear with respect to the light source. Shorter wavelength detects the smaller particle size. The scattered light can be measured by a series of photo detectors placed at different angles. This is known as the diffraction pattern for the sample. As the instrument measures clouds of particles rather than individual ones, it is known as an "ensemble" technique, with the advantage that at smaller sizes (e.g. 1microns) the system is measuring literally millions of particles which gives some statistical significance to the measured results. The particles size distribution (volume percent) of the suspension was carried out in computer-controlled particle size analyzer (Malvern, Mastersizer 2000, UK) via a software program. The powders must not be agglomerated and completely dispersed in the liquid so that they are separated into discrete unattached particles. Powdered samples used to be well dispersed in a liquid medium of known density and viscosity.

3.5.2: Study of Bulk Density and Apparent Porosity

The bulk density and apparent porosity of the sintered specimen were measured by Archimedes' Principle. Here the immersing agent used was kerosene. The dry weight of the sintered specimens was taken. Then the specimens were immersed in kerosene in a beaker. The beaker with samples immersed in it was then put under vacuum in a desiccator so that kerosene fills up the entire open pores present in the sintered specimen.

Then the suspended and soaked weights of the specimens were taken. From these the bulk density and the apparent porosity were calculated.

$$BulkDensity = \left(\frac{W_d \times DensityOfKerosene}{W_{Skd} - W_{Su}} \right) \times 100 \text{ ---------- (1)}$$

$$ApparentPorosity = \left(\frac{W_{Skd} - W_d}{W_{Skd} - W_{Su}} \right) \times 100 \text{ ---------- (2)}$$

W_d= Dry weight of the sample.

W_{Su}= Suspended weight of the sample.

W_{Skd}= Soaked weight of the sample.

3.5.3: Phase Analysis of Calcined and Sintered Pellets.

The phase evolution of calcined powder and sintered sample were studied by X-ray diffraction technique (Philips PANalytical, Netherland) using Cu K_α radiation at 35 KV and 25 mA in the 20-80^0 range and a step size 0.02^0/Sec. The X-ray diffraction (XRD) patterns obtained from the calcined as well as sintered specimen were used to calculate the percentage of tetragonal ZrO_2 (X_t) in each composition by using the Equation below [1]

$$X_t = \frac{I_t(111)}{I_m(111) + I_t(111) + I_m(11\bar{1})} \times 100 \quad \text{…….. (3)} \quad .$$

Where *I (h* k l) = intensity of (h k l) plane, m = monoclinic phase and t = tetragonal phase.

3.5.3.1 Determination of Crystallite Size:

The crystallite size of the calcined powders was determined from X-ray line broadening using the Scherrer's equation [23] as follows:

$$D = \frac{0.9\lambda}{B\cos\theta} \quad \text{----------(4)}$$

Where D is the crystallite size,

λ is the wavelength of the radiation,

θ is the Bragg's angle and

B is the full width at half maximum

3.4.3.2. Lattice Parameter Calculation:

The lattice parameter is the length of the unit cell, which is defined to be the smallest repeat unit that satisfies the symmetry of the crystal. From the X-Ray diffraction data of the calcined samples of various compositions the lattice parameter value was calculated.
Usually we have wavelength λ and the d-spacing [25] is related as the following

$$\lambda = 2d \sin\theta \quad \text{---------- (5)}$$

But also $$d = \frac{a}{\sqrt{\left(h^2 + k^2 + l^2\right)}} \quad \text{---------- (6)}$$

So we get, $$a = \frac{\lambda}{2 \sin \theta} \sqrt{\left(h^2 + k^2 + l^2\right)}$$ ---------- (7)

The lattice parameter for a cubic system is calculated from equation 10

Where

a = Lattice parameter

λ = wavelength of radiation

θ = Half of the 2θ in degrees

h, k, l are the Miller indices.

3.5.4. Dilatometry Study of Pressed Specimens:

The final step of production is sintering. Sintering should be done at a specific temperature, which provides the optimum and maximum densification. Dilatometry study helps to determine the temperature optimum to get better densification and densification behavior. Sintering at lower temperature may not provide better densification. As like, sintering at still higher temperature may lead to fall in density, due to coarsening effect because of grain growth. Thus the sintering behavior study with the help of dilatometer helps determine the sintering temperature zone. The green pellets here were taken for Dilatometry study. The equipment used was NETZSCH DL 402C Dilatometer with an operating range of 25-1600^{o}C. The dimension of green compacts to be put under Dilatometry study was measured. The green compact was then put under test at a temperature range starting from room temperature to 1600^{o}C. The heating rate employed here was 5^{o}C per minute. The behavior was studied with alumina reference.

3.5.5. DSC-TG Analysis.

Thermal decomposition of the calcined powder was monitored by thermogravimetric, TG, and differential thermal analyses, DTA (STA 409, Netzsch), heating at a rate of 10^{0}C min^{-1} up to 1250^{0}C in air. Alpha alumina was used as reference material in DSC runs.

3.5.6. Microstructure Analysis

Prior to Microscopy analysis the samples were polished using rotating disk and Automatic Grinding & Polishing Unit (Buehler, Ecomet 3-Automet 3). The specimen surface was ground on a rotating disk using SiC powder. This process was followed up by grinding the surface on the above-mentioned grinding and polishing unit using 240 grit and 600 grit emery paper disks. The speed of the rotating disk and load at which grinding was carried, varied according to desired status. After this the samples were polished using 6-μm diamond paste on a texmet cloth. Special oil was used as lubrication agent. Final polishing was done using 1 μm diamond paste on a texmet cloth to create a mirror finish. Then the sample was chemically etched by chemical reagent (Distilled water +HF+HNO_3) and followed by a thermal etching. The temperature of thermal etching temperature was 150^0C below the sintering temperature. Surface morphology and grain size of Ceria doped Zirconia sample were observed through Scanning Electron Microscope (JEOL -JSM 6480LV).

3.5.7. Mechanical Properties Analysis

The mechanical properties of ceramics are a complex function of the microstructure. Almost all properties of ceramics are dependent on composition and porosity; strength and fracture behavior apart from these depend on the grain size. Generally, the tensile strength is low and compressive strength is high. This behavior arises because the flaws in the ceramics are effectively closed under compressive stress but rapidly enlarged under tensile stress. Ceramics tend to fail in tension; in a three-point bend (flexural) test failure usually occurs on the side under tensile stress commonly originating from a microstructural, strength-limiting flaw. Tensile strength is a significant mechanical property since the component's reliability and ultimate failure is governed by it. The sintered specimens were characterized for mechanical properties

3.5.7.1. Hardness measurement:

Hardness is usually defined as resistance to penetration. It is a measure of the yield stress of the ceramic. Usually the measured value of hardness is load-dependent. Especially at low loads the measured values of microhardness tend to increase. This reflects an effect of a ratio of the impression size to a characteristic microstructural dimension such as grain size, pore size and distribution, inclusions, and the range of residual stresses. The microhardness also depends on the relationship of surface properties vs. bulk properties and on

environmental interactions. At high loads, such as several kilograms, the measured hardness of ceramics decrease due to the fracture of the material during indentation.

Hardness is a measure of a reaction of a material to the type of disturbing force imposed (different hardness test results for different techniques) and relates to:

- Ease of dislocation movement e.g. to shear modulus *G* and yield stress
- The type of atomic bonding
- The presence of impurities in solid solution or at grain boundaries and/or as precipitates, or inclusions
- The microstructure (grain size and texture, porosity), phase composition and residual stresses

.

Fig.3.6 Vicker's Hardness tester

The sintered pellets were polished in the same manner as done for SEM analysis (as discussed in section 3.12.). After cleaning the specimens with acetone in a Ultrasonic bath (TEKSONICS make) the specimen were taken for indentation at different loads using Vicker's Hardness Tester

The samples were indented by a diamond indenter with 49N and 98N load and 20seconds dwell time. The hardness of the materials was calculated from the size of the impression produced under load by a pyramid-shaped diamond indenter. The indenter employed in the test is a square based pyramid whose opposite sides met at the apex at an angle of 136^{o}. The size of the impression (diagonals) was measured with the aid of a calibrated optical microscope (make ZEISS). The hardness of various samples was measured by using the following equation [30]

$$H_v = 1.854\left(F/D^2\right) \quad \text{..... (8)}$$

F being the applied load measured in kgf

D^2 is the area of the indentation (measured in mm^2)

3.5.7.2. Diametrical Compressive Strength/ Brazilian Disk test analysis:

Diametrical Compression test is a test to determine the limit of performance of a material to stress. This test is also known as Brazilian Disk Test. This mechanical testing technique is used in many technological fields from concrete to ceramics: to metal composites to materials in dentistry. In this method a local tensile stress is induced in the transverse direction of the applied compressive stress. Usually specimen in the form of disk (pellets) is used. This test helps us to measure the limit force required to cause failure, which is used in estimation of tensile strength.

The diametral compressive strength was measured using Hertz equation [24]: -

$$\sigma_{comp.} = \left(\frac{2P}{\pi DT}\right) \text{---------- (9)}$$

Where; $\sigma_{comp.}$ is the compressive strength

P is the breaking load

D is the diameter of the sintered compact

T is the thickness of the sintered compact

The advantages of Brazilian disk test are-

- Its simple geometry,
- Ease of specimen preparation
- Quickness of testing.

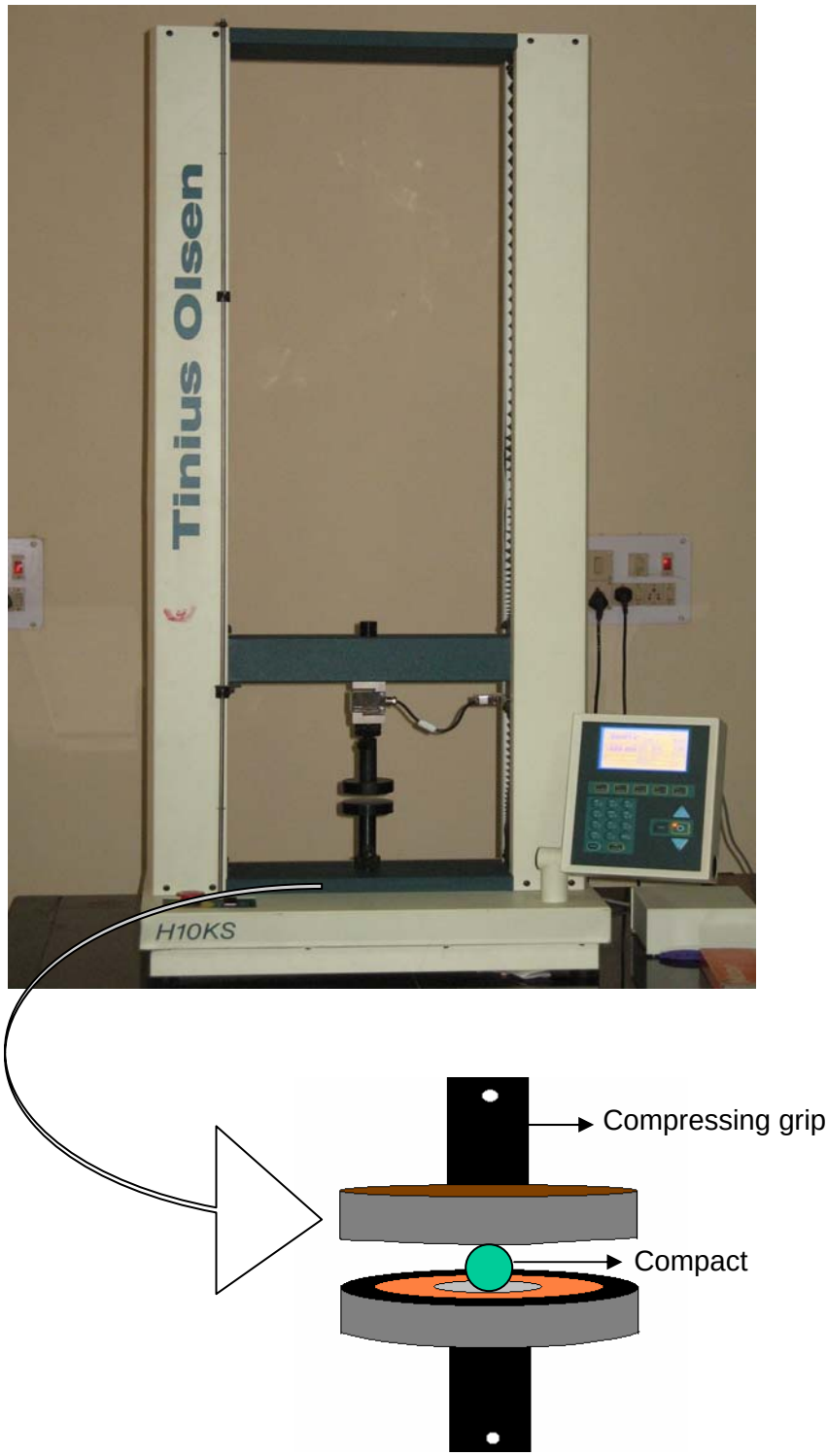

Fig. 3.7 Arrangement for Brazilian Disk Test

3.5.7.3. Flexural Strength at Ambient temperature:

A determination of the flexural strength is frequently necessary as a part of the design of structural ceramics to check compliance with established specifications or to provide information necessary to the design of an engineering structure. It is the ability of a bar or slab to resist failure in bending. The flexural strength is expressed as "Modulus of Rupture" (MR) in MPa. Flexural Strength is about 10 to 20% of compressive strength. However, the best correlation for specific materials is obtained by laboratory tests according to ASTM methods [24].

Three samples of each batch were taken to determine the flexural strength at each test and the average values have been reported here. Flexural strength was determined by standard three-point bending method in an instrument {Instron Universal Testing Machine (Hounsfield H10KS, U.K)}. The parameters for the three point bend test were- span length of 30mm with cross head speed of 0.2mm/min. The edges of the rectangular bars were ground on grinding discs of 600grit using polishing machine, Automet-3 and Ecomet-3(made Buehler) to give a parallel and smooth surface. Flexural strength was calculated from the following equation [24]:

$$\sigma_{flexural} = \left(\frac{3PL}{2WD^2} \right) \text{ ---------- (8)}$$

Where; P = fracture load

L = Span length/ distance between the rollers

W = width of the sample;

D = Thickness of the sample at the fracture plane**.**

3.5.7.4. Fracture Toughness Test:

The fracture toughness was measured in 3point bending using SENB method {Instron Universal Testing Machine (Hounsfield H10KS, U.K)}. The edges of the rectangular bars of were ground on grinding discs of 600grit using polishing machine, Automet-3 and Ecomet-3(made Buehler) to give a parallel and smooth surface. Then notch was made in the sample by diamond cutter. The sample bars were subjected to fracture toughness measurement. The parameters for the three point bend test were span length of 30mm with cross head speed of 0.2mm/min.

Chapter 4

RESULTS AND DISCUSSION

Ceria stabilized Zirconia powder was prepared by co-precipitation method. The phase analysis in calcined as well as sintered samples was characterized by XRD. Sintered samples were characterized by XRD, density measurement and microstructure analysis (SEM). Subsequently, compressive strength, flexural strength, hardness and fracture toughness were evaluated and analyzed with respect to microstructure.

4.1. TG-DSC Analysis:

TG and DSC curves of the raw powder prepared by co-precipitation method are shown in Fig.4.1 (a) and Fig.4.1 (b). The weight loss is substantial up to 850^0C and is negligible beyond this temperature. Total weight loss is about 23.12% in case of 10 mol% Ceria doped Zirconia and about 20.54% in case of 12 mol% Ceria doped Zirconia It was proposed earlier [4,14] that while co-precipitating Zr^{4+} and Ce^{3+} cations, cerium enters into solid solution in a trivalent state. However, it is generally known that when cerium hydroxide is precipitated, it slowly oxidizes in contact with air. The continuous changes observed in the color of the precipitate during subsequent processing just after precipitation, suggests that both Ce^{4+} and Ce^{3+} may be present in the precipitated hydroxides. The weight loss observed is attributed to the thermal decomposition of the precipitated hydroxides and to the residual water.

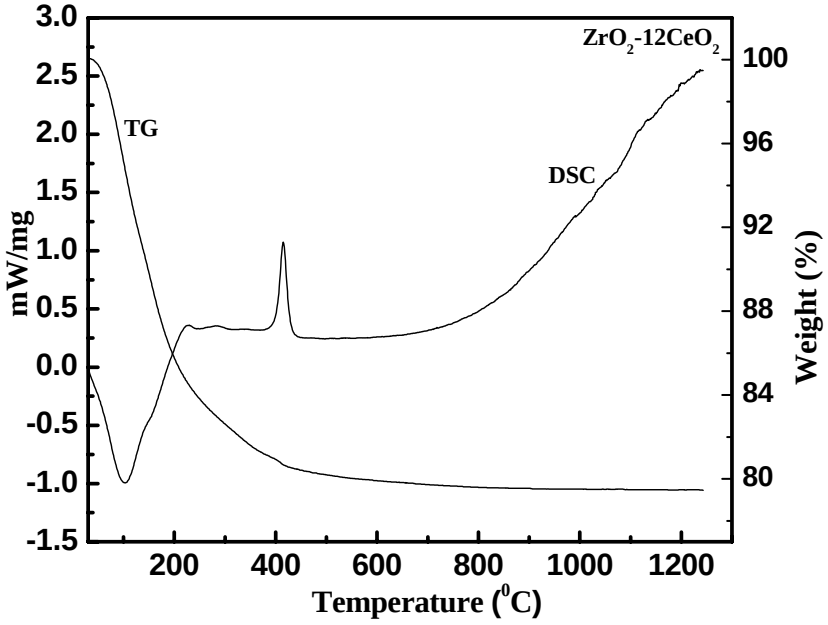

Fig. 4.1 (a): TG-DSC Curve of 10mol% Ceria Zirconia Raw Powder

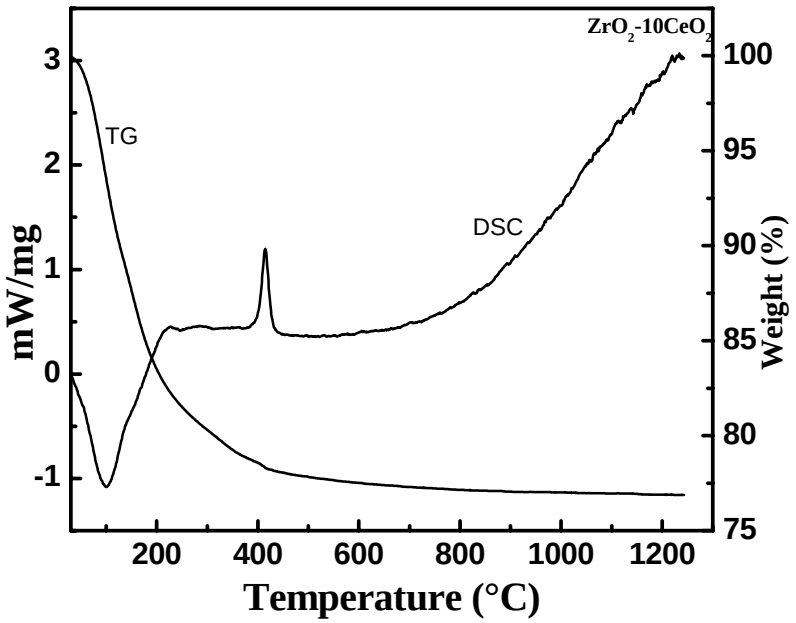

Fig. 4.1 (b): TG-DSC Curve of 12mol% Ceria Zirconia Raw Powder

The DSC curve shows exothermic peaks centered at 414.8^0C and 415.1^0C for 10 and 12 mol % Ceria doped Zirconia respectively. The DSC curve also shows a low-temperature endothermic peak at 99.2^0C and 103^0C for 10 and 12 mol% Ceria doped Zirconia powder respectively. This endothermic peak is attributed to loss of water and alcohols. The exothermic peak is due to the crystallization of the solid solution [10].In present work calcination temperature and time were chosen as 850^0C and 4 hours respectively, as the samples show no further weight loss around this temperature (i,e.850°C).

4.2: Phase analysis in calcined powder by XRD.

Phase analysis of ceria stabilized zirconia system has been done as a function calcination temperature. Fig.4.2 (a) and Fig 4.2 (b) show the XRD pattern of 10 mol% and 12 mol% ceria stabilized zirconia respectively, calcined at different temperatures such as 650°C,750°C,850°C and 950°C.The XRD pattern of the calcined powder samples were analysed for phase evolution.

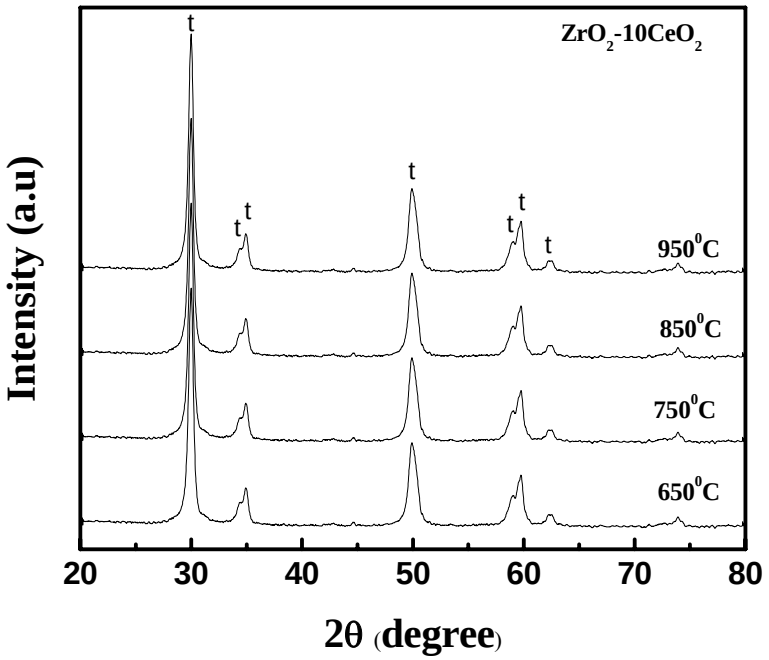

Fig. 4.2: (a): XRD pattern of the 10 mol% Ceria doped Zirconia powder calcined at different temperatures.

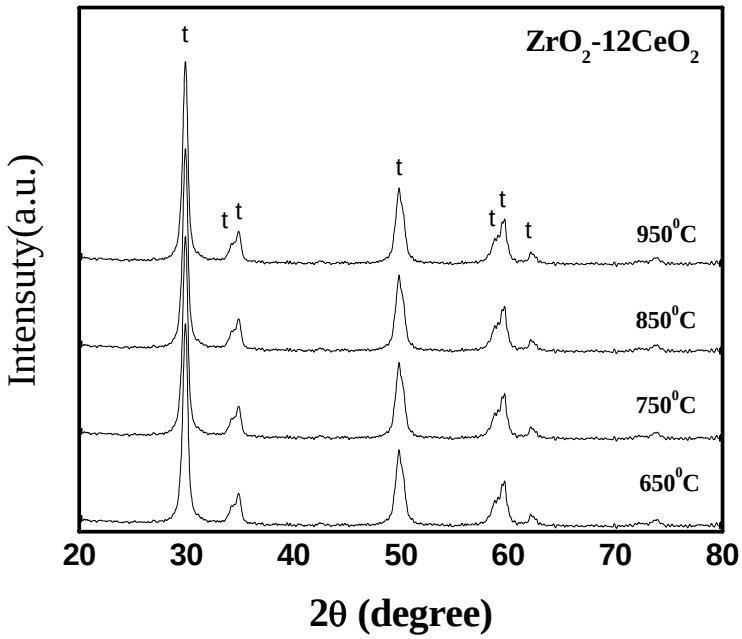

Fig. 4.2 (b): XRD pattern of the 12 mol% Ceria doped Zirconia powder calcined at different temperatures

The powder shows fine crystallite size of the Ce-TZP even after calcined at 650°C as exhibited by broadening peaks. The phase evolution of calcined powders could be deliberated with reference to the diffraction pattern of a tetragonal phase (ICDD File card no.73-1441). Calcination at higher temperatures did not change the peak position, but the intensity of the diffraction peaks of the tetragonal phase gradually increased as the calcination temperature increased to 950^0C. The diffraction peaks become stronger and sharper when calcined at 950^0C. The sharper and higher intensity peaks confirmed the increase in crystallite size. From the Scherer's formula [24] (Equation 4 as mentioned in Section 3.4.3.1) the average crystallite size was calculated from peak broadening. The crystallite size was found to range between 28nm for lowest calcination temperature to 38nm for highest calcination temperature for 10 mol % Ceria doped Zirconia. For 12 mol % Ceria doped Zirconia powder crystallite size was found to range between 27nm for lowest calcination temperature to 37nm for highest calcination temperature. Fig. 4.2 (c) shows a plot of crystallite size with respect to different calcination temperatures. The measured crystallite size for samples calcined at different temperatures is given in Table 4.1.The crystallite size was found to increase with increasing calcination temperature.

Both the 10 and 12mol% Ceria stabilized Zirconia are having tetragonal phases at all temperatures. But the crystalline size is different for different temperatures.

The crystallite size was calculated using Scherer formula [25]

Table 4.1: Crystallite Size at different temperatures

Calcination Temperature (^{0}C)	Crystalline Size (nm)	
	10 Ce-TZP	12 Ce-TZP
650	28	27
750	30	28
850	33	32
950	38	37

.

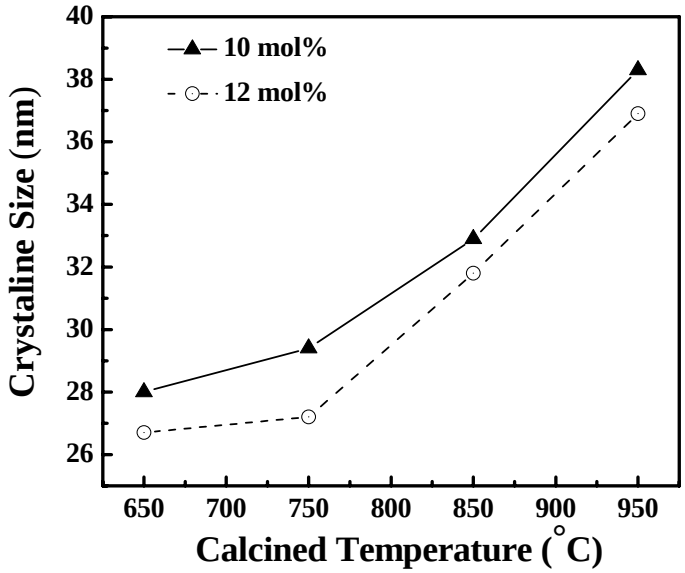

Fig 4.2 (c): Crystallite size as a function of calcination temperature

It has been seen that the crystallite size increases with increases in temperatures [4].

4.3: Particle Size Analysis:

The distribution of particle sizes after calcinations of the precipitate at 850°C for 10 mol% and 12 mol % ceria doped zirconia respectively are shown in fig.4.3. (a) and fig.4.3 (b) respectively. This curve does not represent the particle size distribution, as certain powder agglomerates were present which were not be properly dispersed during the process of sample preparation for this characterization. However, this curve does indicate the average degree of powder agglomeration.

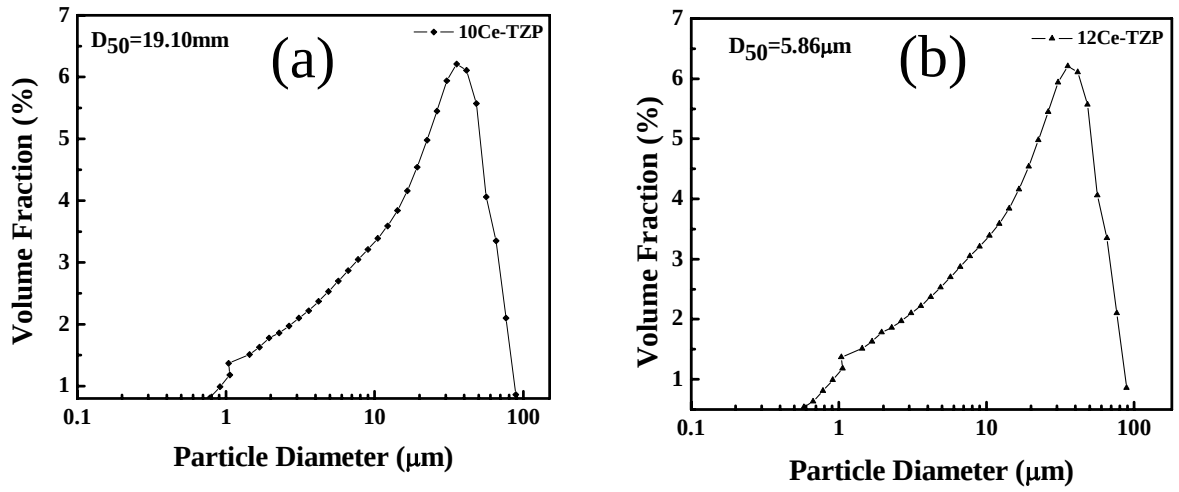

Fig 4.3 Agglomerate size distribution of ceria doped zirconia powder calcined at 850°C. (a) 10 mol%. (b) 12 mol%

The average particle/agglomerate size obtained at 50% cummulative volume is 19.4μm for 10 mol% Ceria doped Zirconia and 5.84 μm for 12 mol% Ceria doped Zirconia powder. The particle size could be observed by scanning Electron microscope. Even though the results on laser scattering and scanning electron microscopy give information regarding the distribution and shape of particles/agglomerates, they are not sufficient for the evaluation of the strength of these agglomerates.

4.4. Dilotometry Analysis:

The linear shrinkages of 10 mol% and 12 mol% Ce-TZP powder compact are shown in Fig. 4.4 (a) and Fig.4.4 (b) respectively. Higher shrinkage occurs between 902^0C and 1200^0C. For temperatures higher than 1200^0C the grain growth mechanism predominates. Total shrinkage of the compact is about 22-23% and the temperature of maximum shrinkage is 1150°C as determined by the derivative curve. Previous dilatometric experiments [12, 13] performed on specimens prepared by the same synthesis technique exhibit a total shrinkage less than 17% at 1400 ^{0}C. These contrasting results can be attributed to the better powder properties reported here.

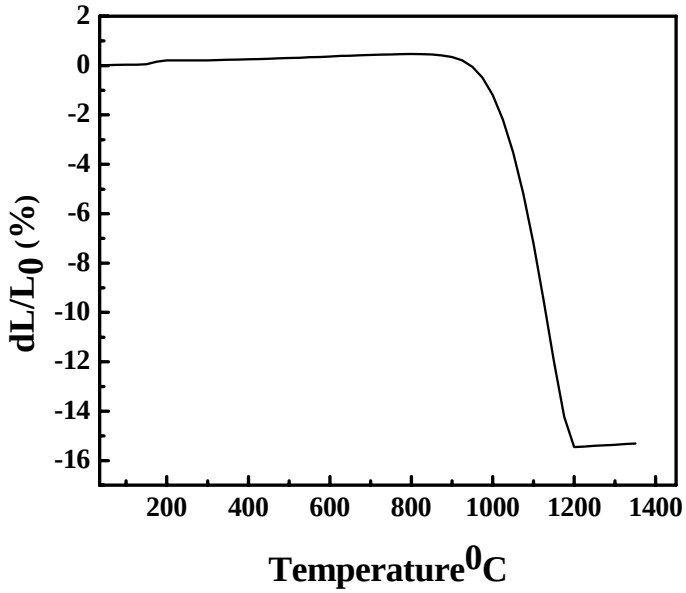

Fig. 4.4 (a): Non isothermal densification behavior of 10 Ce-TZP

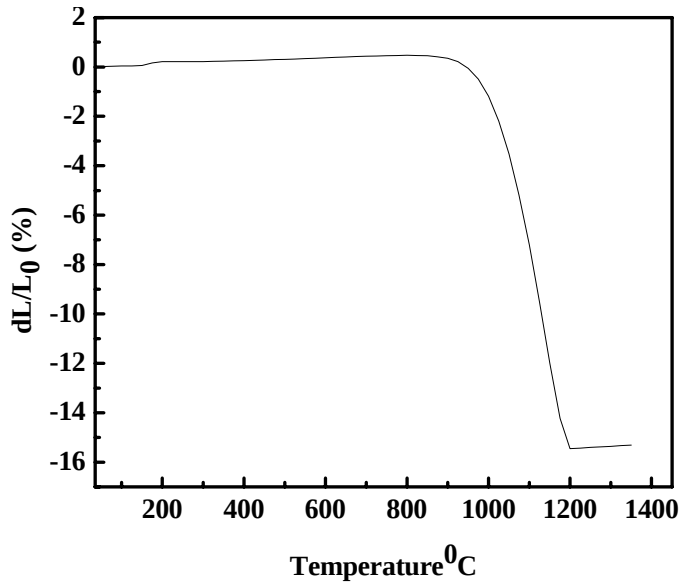

Fig. 4.4 (b): Non isothermal densification behavior of 12 Ce-TZP

4.5. Phase analysis in sintered samples:

Fig.4.5 (a) and Fig.4.5 (b) show the XRD pattern of 10 mol% and 12 mol% ceria stabilized zirconia in ordinary air atmosphere sintered at three different temperature such as 1400°C, 1500°C and 1600°C where as Fig.4.5 (c) and Fig.4.5 (c) show the XRD pattern of 10 mol% and 12 mol% ceria stabilized zirconia in ordinary nitrogen atmosphere sintered at same temperature are reported. The sharp well defined peaks show the high crystalline nature of the synthesized phase without any impure phase. Thus the phases obtained remains stable even at high temperature sintering .This has been possible due to the very nature of the synthesis technique adopted in this investigation.

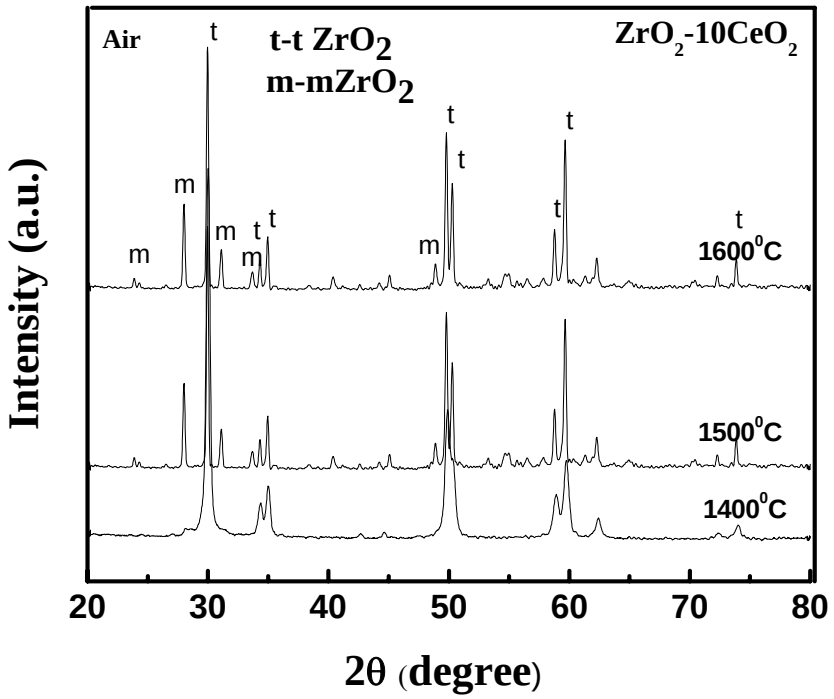

Fig.4.5: (a) XRD pattern of 10mol%Ceria doped zirconia samples sintered in air atmosphere at different temperatures

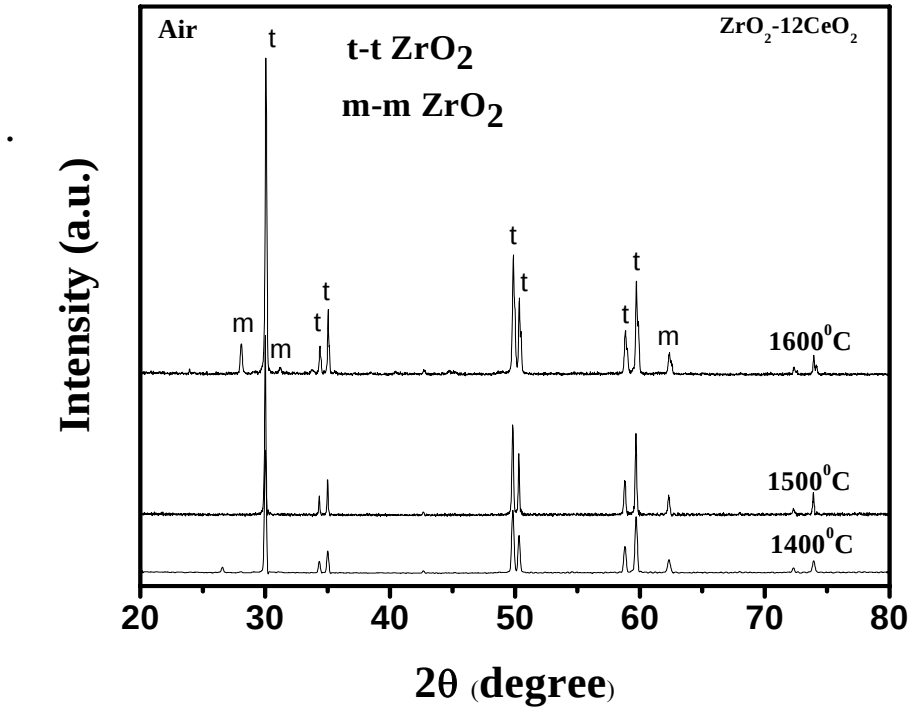

Fig.4.5 (b) XRD pattern of 12mol%Ceria doped zirconia samples sintered in air atmosphere at different temperatures.

The major phases observed after sintering in air were that of tetragonal (101) (110) (200) and monoclinic (-111), (111), (220).only tetragonal phase appeared in both 10 and 12 Ce-TZP samples, but some monoclinic phase is present also in both the samples at 1600^0C.This is due to fact that at high temperature tetragonal to monoclinic transformation occurs due to increase in grain size.

Fig 4.5 (c) and Fig.4.5 (d) show the XRD pattern of the samples sintered in Nitrogen atmosphere. At 1400^0C, 10Ce-TZP shows tetragonal and little amount of monoclinic phases, but 12Ce-TZP shows pure tetragonal phases. At high temperature, besides t-ZrO_2 and monoclinic phases additional phases were found in nitrogen sintered sample. The additional phase was found to be (Zr,Ce)O_2 solid solution [5,22].The solid solution having tetragonal crystal structure as reveled by JCPDS card (82-1398 and 38-1437).It was found that sample cracked after sintering in nitrogen atmosphere.

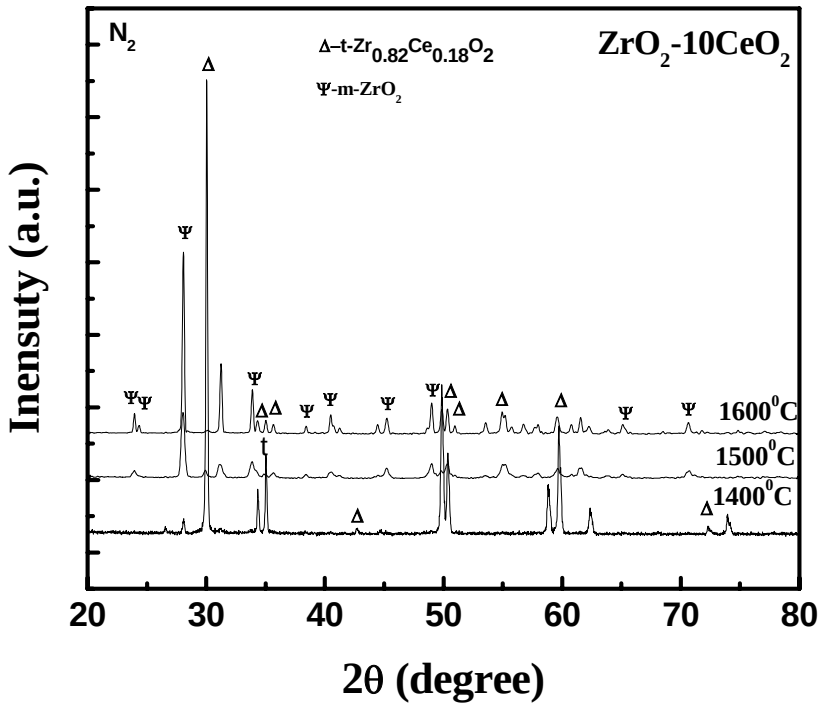

Fig.4.5 (c) XRD pattern 10mol%ceria doped zirconia samples sintered in N_2 atmosphere.

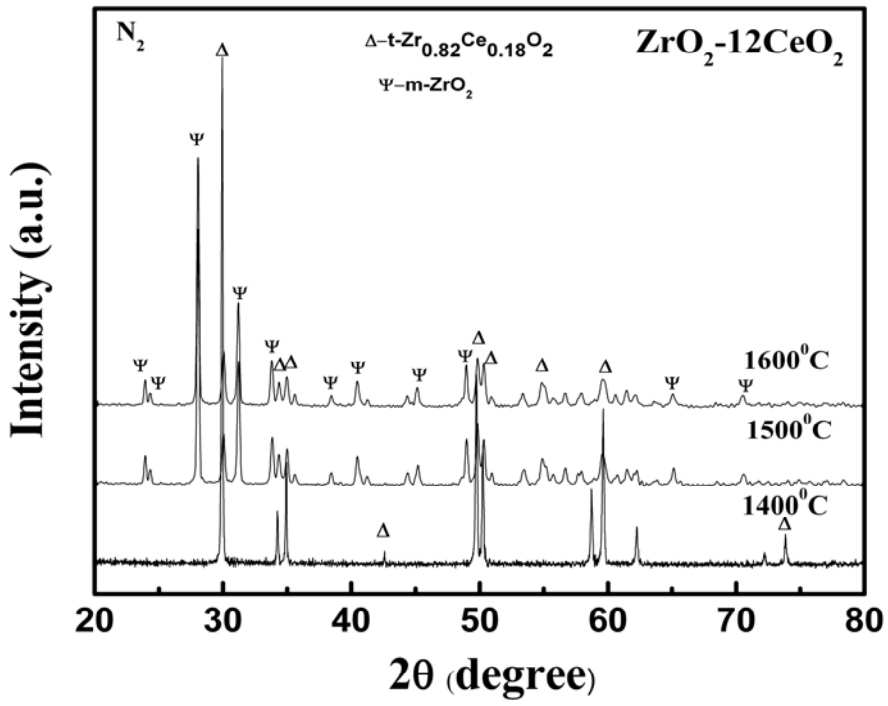

Fig.4.5 (d) XRD pattern of 12mol%Ceria doped zirconia samples sintered in N_2 atmosphere.

4.6. Densification Study

Density of the 10 and 12 mol% ceria doped zirconia samples sintered in air and nitrogen atmosphere at 1400^0C to 1600^0C / 4 hrs has been shown in fig.4.6 (a) and fig.4.6 (b) respectively. For sintering in air, the density increase in 10 mol% ceria stabilized zirconia with temperature increases up to 1550°C,beyond which the density decreases gradually. This is due to increases in micro crack present in the sample. But in case of 12 mol % ceria stabilized zirconia density increases slowly up to 1500°C with higher increases up to 1550°C beyond which the increase is less.

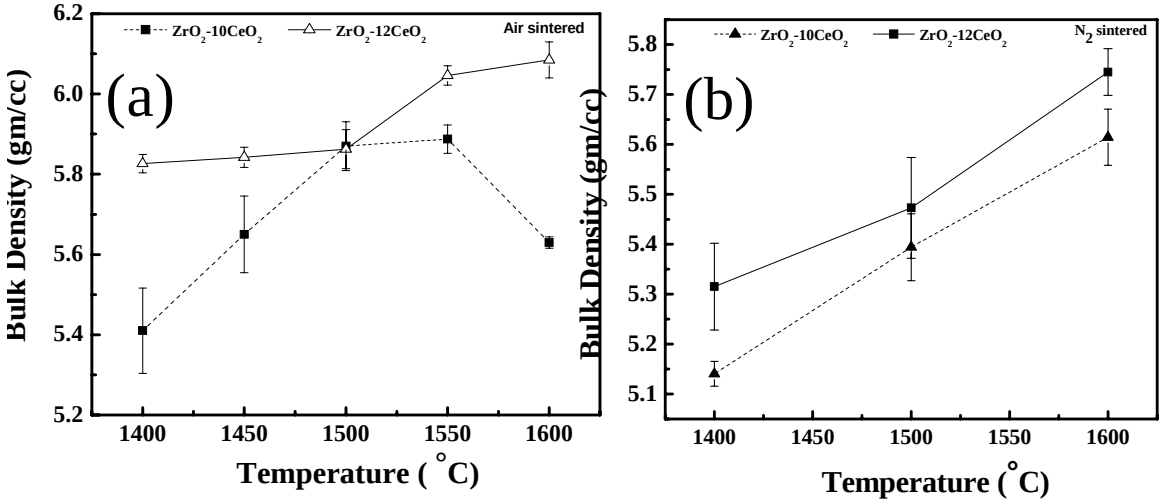

Fig.4.6: Density of Ceria doped zirconia at temperature 1400 to 1600^oC

(a) Oxidized atmosphere (b) Nitrogen atmosphere

The same samples were sintered in nitrogen atmosphere, it was observed that the density increases at all temperature up to 1600°C.The density being higher for 12 mol% ceria stabilized zirconia than 10 mol% ceria stabilized zirconia.

The theoretical density of the sample has also been calculated on the basis of percentage of tetragonal and monoclinic phase present in sintered sample. The results are reported in the Table 4.2 and Table 4.3 for air and nitrogen atmosphere respectively

Table 4.2: Theoretical and Bulk Density of sample sintered in air.

Sample	t-ZrO_2	m-ZrO_2	Theoretical .Density(gm/cc)	Bulk Density(gm/cc)
10/1400	78.17	21.83	6.061	5.41
10/1500	47.99	52.01	5.995	5.61
10/1600	11.82	88.18	5.9178	5.81
12/1400	100	0	6.11	5.82
12/1500	100	0	6.11	5.86
12/1600	87.35	12.65	6.00	5.98

Table 4.3: Theoretical and Bulk Density of sample sintered in N_2.

Sample	t-ZrO_2	m-ZrO_2	Theoretical .Density(gm/cc)	Bulk Density(gm/cc)
10/1400	93.19	6.81	6.08	5.14025
10/1500	7.24	92.76	5.9064	5.39419
10/1600	0	100	5.89	5.6145
12/1400	100	0	6.10	5.3153
12/1500	12.43	87.57	5.9082	5.4728
12/1600	8.56	91.44	5.9079	5.745

It has been shown that density is better in case of samples sintered in air oxidised atmosphere than nitrogen atmosphere. The density attained is 98% of theoretical density at 1600^0C**.**

4.7. Mechanical Properties:

Mechanical strength of ceramic materials depends mainly on two parameters. One is the intrinsic property of the phases present and the microstructure of the material. In multiphase material, microstructure of the materials, i.e. the amount and distribution of the phases play a crucial role in determining the mechanical strength. The test methodologies also play significant role on the strength values. According to the application, the material

can experience fully compressive strength, tensile strength and/or intermediate of these. In this chapter the hardness, compressive strength and flexural strength tests have been carried out. Attempts have been made to correlate the compressive strength with the bending strength values. Finally, the fracture toughness has been evaluated by 3 point bending test at room temperature.

4.7.1: Hardness Test (Vickers hardness)

Fig 4.7.1 shows the Vicker Hardness of the 10 and 12 mol% Ce-TZP samples sintered in air atmosphere. The hardness of 12 mol% ceria TZP increases with increasing sintering temperature up to 1550°C.but decreases beyond that temperature. For 10 mol% Ce-TZP, the hardness increases up to 1500°C, then variation of hardness resulted as shown in figure.

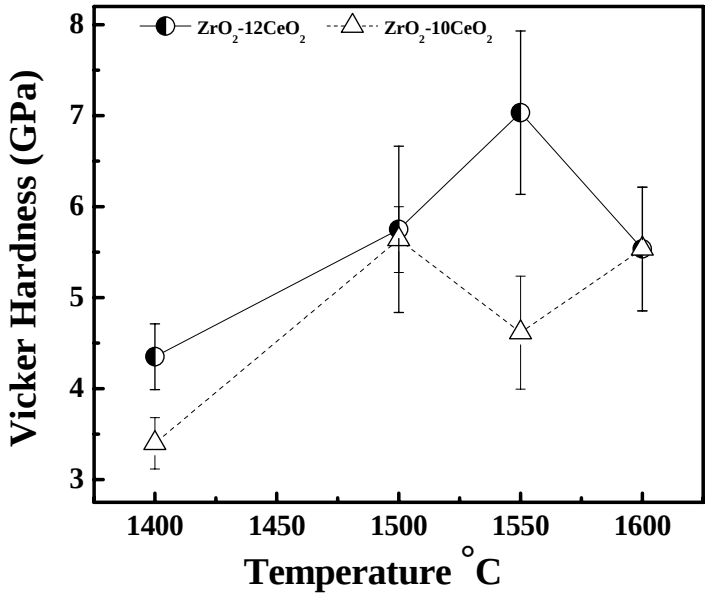

Fig.4.7.1: Hardness as a function of sintering temperature.

4.7.2. Diametrical Compression Test / Brazilian Disk Test:

Strength tests such as the tension test, the diametrical compression test/Brazilian disk test [26], and the simple compression test determine the limit of performance of a material to stress. As such, strength criteria can be built using a combination of the local principal stresses.

Fig.4.7.2 (a) and Fig.4.7.2 (b) shows the Compressive strength for the both 10 mol% and 12 mol% Ce-TZP sintered in air and nitrogen atmosphere respectively. The compressive strength increases up to 1500°C and then decreases for air sintered sample. It was observed

that the compressive strength of 12 Ce-TZP is more than 10 Ce-TZP. In general is high because the flaws in ceramics in this case are close [27]

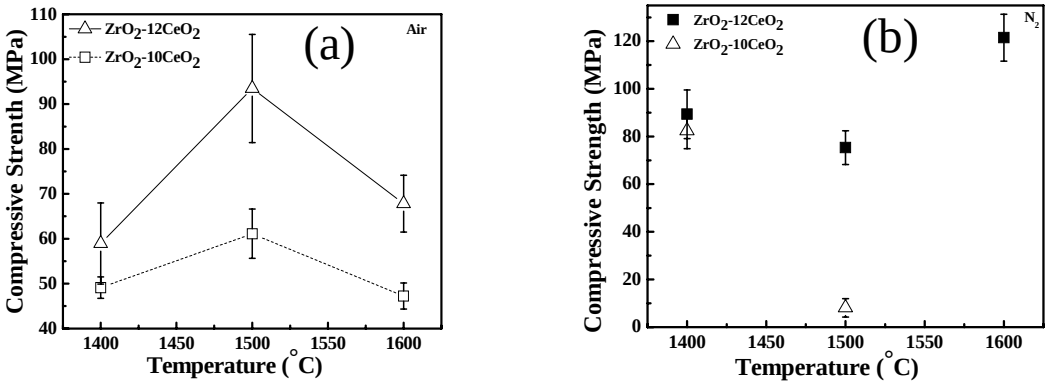

4.7.2: Compressive Strenth of ZrO_2 -10 and 12 mol% CeO_2 sintered in (a) air and (b) Nitrogen atmosphere

4.7.3. Flexural Strength

The three point bending strength for Ceria stabilized zirconia samples sintered in air and nitrogen atmosphere was measured as a function of sintering temperatures shown in fig.4.7.3 (a) and fig.4.7.3 (b) respectively. The strength increased with increase in Ceria content with the higher strength exhibited for 12 mol% Ceria addition. However, the strength was more for 1600^0C sintered samples and less for 1400^0C sintered samples. The flexural strength is found to increases in both the samples with increases in sintering temperature due to better densification.

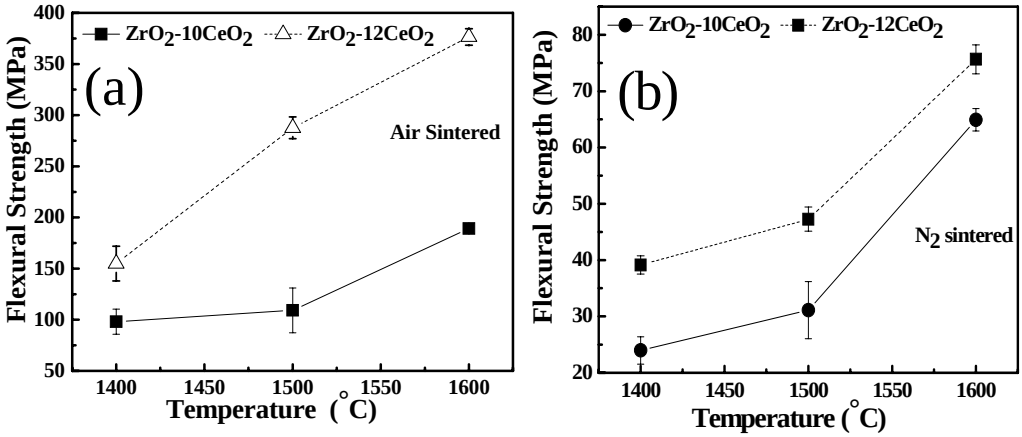

4.7.3: Flexural Strength of Ce-TZP Sintered in (a) air and (b) nitrogen atmosphere

4.7.4: Fracture Toughness:

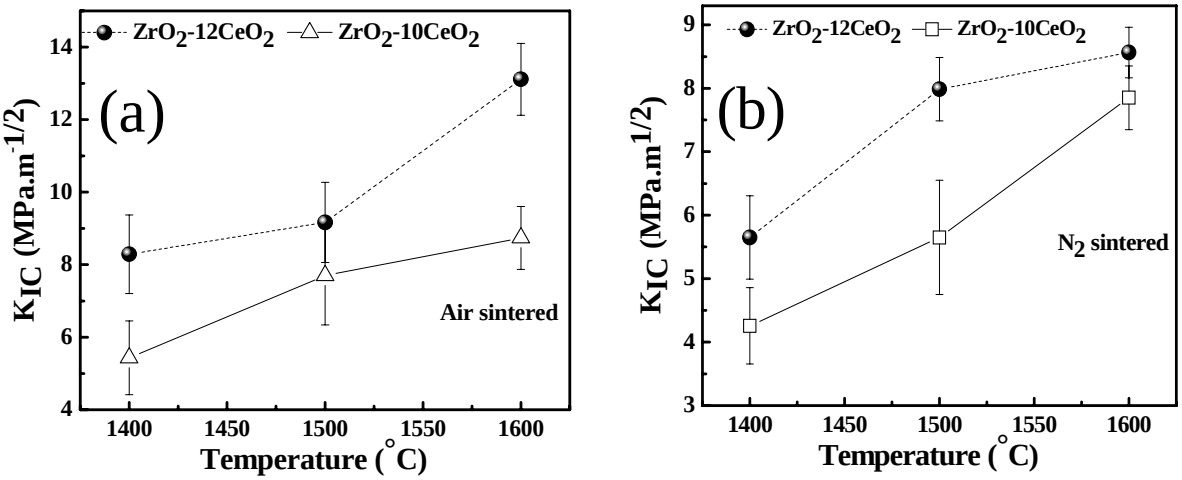

Fig. 4.7.4 (a) Fracture toughness Ceria stabilized Zirconia Sample in air atmosphere. (b) Fracture toughness in N_2 atmosphere

Fracture toughness was calculated using SENB method by INSTRON Model-Hounsfield H10KS, U.K.Fig.4.7.4 (a) and fig.4.7.4 (b) show the fracture toughness of 10 and 12 Ce-TZP sintered in air and nitrogen atmosphere respectively. It was found that for air sintered sample, the fracture toughness is much higher than nitrogen sintered sample. A maximum toughness of 13 $MPam^{-1/2}$ was observed for air sintered sample for 12 mol% CeO_2-ZrO_2 but for nitrogen sintered sample a maximum of 8.7 $MPa.m^{-1/2}$ was achieved for the same sample. The fracture toughness of nitrogen atmosphere sintered samples is less which can be explained in terms of microstructure, crystallite size and phase composition in sintered sample. The microstructure of nitrogen sintered sample shows porous and the XRD result revealed that $(Zr,Ce)O_2$ solid solution phase present in the nitrogen sintered sample which degrade the mechanical properties.

4.8. Microstructure Analysis

Fig. 4.8 (a) and Fig. 4.8 (b) shows the SEM of 10 and 12 mol% Ce-TZP sample sintered in air atmosphere at 1500^0C. It clearly indicates that pores are present in the inter and intra granular region. There is no secondary phases present in the sample which is closely related to XRD results.

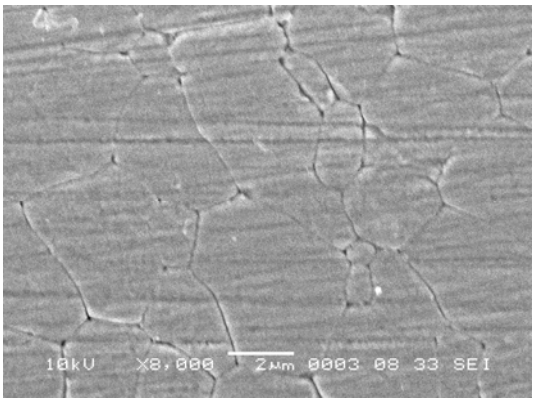

Fig.4.8 (a) SEM of 10 mol% CeO_2-ZrO_2 sintered in air atmosphere.

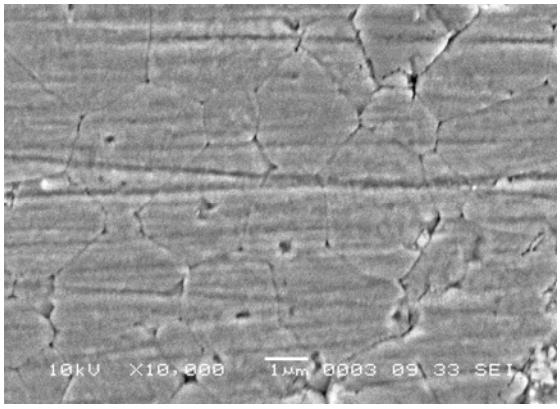

Fig.4.8 (b) SEM of 12 mol% CeO_2-ZrO_2 sintered in air atmosphere.

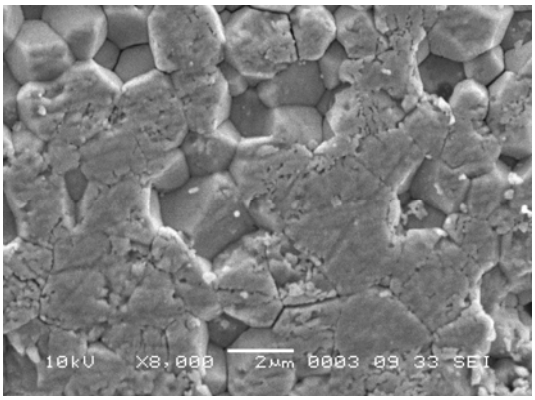

Fig.4.8 (c) SEM of 10 mol% CeO_2-ZrO_2 sintered in nitrogen atmosphere.

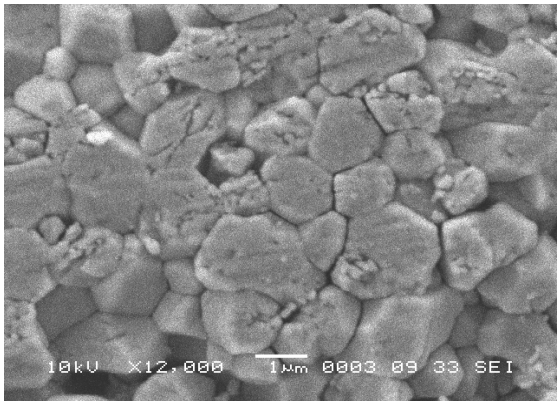

Fig.4.8 (d) SEM of 12 mol% CeO_2-ZrO_2 sintered in nitrogen atmosphere.

Fig. 4.8 (c) and Fig. 4.8 (d) shows the SEM of 10 and 12 mol% Ce-TZP sample respectively sintered in nitrogen atmosphere at 1400^0C. It has been observed that grains are irregular and polyhedral in shape.

The material sintered in air atmosphere seems to be more dense compared to sample sintered in nitrogen atmosphere due to the presence of pores and cracks in nitrogen sintered samples.

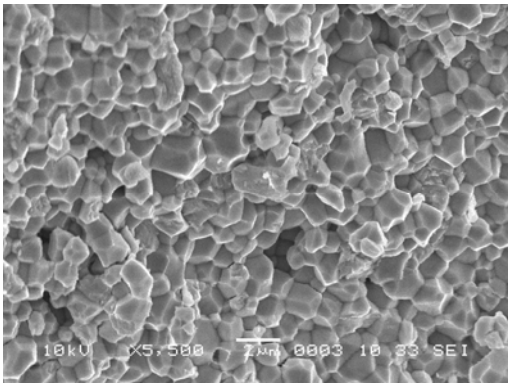

Fig.4.8 (a) SEM of fracture surface

A typical SEM micrograph of fractured surface is shown in Fig. 4.8 (e). It shows an intergranular fracture and regular polygonal grain shape.

Conclusions

Ce-TZP (10 and 12 mol %) powder were prepared by precipitation from aqueous precursors $ZrOCl_2$ (for ZrO_2) and Ammonium Ceric Nitrate (for CeO_2). The precipitated powder were washed followed by calcinations at 850°C.The DSC/TG study of the precipited dried powder show an endothermic peak in the low temperature range (~100°C) due to removal of absorbed water and exothermic peak at higher temperature (~400°C) due to crystallization of ZrO_2.XRD of calcined powder of both composition (10 and 12 mol %) shows tetragonal zirconia up to 950°C. At higher temperature calcined samples, the tetragonal peak becomes more intense which indicate an increase in crystallite size (28-38nm.). The calcined powder of both compositions were compacted into cylindrical pellets and rectangular bars and sintered at 1400°C, 1500°C, 1600°C both in air as well as nitrogen atmosphere. The air sintered samples shows high sintered density and high volume fraction of tetragonal phase where as nitrogen sintered sample show low density and tetragonal phase retention is also very low. The nitrogen sintered sample show $(Zr,Ce)O_2$ solid solution. The microstructure of N_2 sintered sample show porous structure in comparison to air sintered sample which were dense. For air sintered sample, the strength and toughness is highest in 1600°C.Relatively large grain size was observed at 1600°C due to more stress induced t-m transformation.

References:

[1]. Stevens R.*Introduction to Zirconia,Elektron Publication*,2nd Edition.page15-38

[2]. N. S. Jacobson, "*Thermodynamic Properties of Some Metal Oxide-Zirconia Systems*", NASA Technical Memorandum 102351

[3]. Sim, S.M.; and Stubican, V.S.: Phase Relations and Ordering in the System ZrO_2-MgO. J. Am. Ceram. Soc., vol. 70, no. 7, July 1987, pp. 521-526.

[4]. Stubican, V.S.; and Hellman, J.R.: *Phase Equilibria in Some Zirconia Systems. Science and Technology of Zirconia*,(Advances in Ceramics, vol. 3), A.H. Heuer and L.W. Hobbs,eds., American Ceramic Society, Columbus, OH, 1981, pp.25-36.

[5]. Stubican, V.S.; Hink, R.C.; and Ray, S.P.: *Phase Equilibria and Ordering in the System ZrO_2-Y_2O_3,* J. Am. Ceram. Soc., vol. 61, no. 1-2, Jan.-Feb. 1978, pp. 17-21.

[6]. Marder J. M.,Mitchell T.E. and Heuer A.H.,*Precipitation from cubic ZrO_2 solid solution".Acta Metall,* **31**,(3) 387,395,1983

[7]. Muroi, T.; Echigoya, J.I.; and Suto, *Phase Diagram of ZrO_2-CeO_2 Ceramics.* Trans. Jpn. Inst. Met.,vol. 29, no. 8, Aug. 1988, pp. 634-641.

[8]. S. K. Tadokoro and E. N. S Muccillo, "*Physical characteristics and sintering behavior of ultra fine zirconia-ceria powder*", J. *Euro. Ceram. Soc.*, **22** (2002) 1723.

[9]. J. Vleugels, C. Zhao and O. V. D. Biest, "*Toughness enhancement of Ce-TZP by annealing in argon*", *Scrip. Mater, 50* (2004) 679.

[10]. S. C. Sharma, N. M. Gokhale, R. Dayal and R. Lal, *Bull. Mater. Sci..*, **25** (2002) 15.

[11]. M. Matsuzawa, M. Abe, S. Horibe and J. Sakai, "*The effect of reduction on the mechanical properties doped tetragonal zirconia ceramics of CeO_2*", *Acta Mater.*, **52** (2004) 1675.

[12]. A. Tiefenbach, S. Wagner, R. Oberacker and B. Hoffmann, "*Measurement of the t-m and m-t transformations in Ce–TZP by dilatometry and impedance spectroscopy*", *J. Eur. Ceram. Soc.*, **22** (2002) 337.

[13]. Z. X. Yuan, J. Vleugels and O. V. D. Biest, "*Synthesis and characterization of CeO_2 coated ZrO_2 powder-based TZP*", *Mater. Lett.* **46** (2000) 249.

[14]. Y. Zhou and M. N. Rahamanz, "*Effect of redox reaction on the sintering behavior of cerium oxide*", *Acta Mater.*, **45**, (1997) 3635.

[15]. C. Zhao, J. Vleugels, C. Groffils, P. J. Luypaert and O.V. D. Biest, "*Hybrid sintering with a tubular susceptor in a cylindrical single-mode microwave furnace*, *Acta Mater.*, **48** (2000) 3795.

[16]. T. Sato , K. Dosaka, M. Ishitsuka , E. M. Haga and A. Okuwaki, "*Sintering behaviour of ceria-doped tetragonal zirconia powders crystallized and dried using supercritical alcohols*", *J. Alloys and Comp.*, **193** (1993) 274.

[17]. H. E. Attaoui, M. Saadaoui, J. Chevalier and G. Fantozzi, "*Static and cyclic crack propagation in Ce-TZP ceramics with different amounts of transformation toughening*", *J. Eur. Ceram. Soc.* **27** (2007) 483.

[18]. G. A. Gogotsi,V. P. Zavadaa and M. V. Swain, "*Mechanical Property Characterization of a 9 mol% Ce-TZP Ceramic Material - I. Flexural Response*", *J. Eur. Ceram. Soc.* ,15 (1995) 1185.

[19]. S. Gutzov and M. Lerch, "*Nitrogen incorporation into pure and doped zirconia*" Ceram. Inter. **33** (2007) 147.

[20]. H. M. Ondik, H. F. McMurdie, editors. "*Phase diagrams for zirconium and zirconia systems*". Westerville, OH: *American Ceramic Society*; 1998. P.264.

[21]. H. K. Schmid, *J. Am. Ceram. Soc.*, **74** (1991) 387.

[22]. S. Lathabai, **"***The Effect of Grain Size on the Slurry Erosive Wear of Ce-Tzp Ceramics*"**,** *Scripta Mater*. **43** (2000) 465.

[23]. W. Chen, F. Li, J. Yu, L. Liu and H. Gao, "*Rapid synthesis of mesoporous ceria–zirconia solid solutions via a novel salt-assisted combustion process*", *Mater. Res. Bull.*, **41** (2006) 2318.

[24]. L. F. C. P. Lima, A. L. E. Godoy and E. N. S. Muccillo, "*Elastic modulus of porous Ce-TZP ceramics*", *Mater. Lett.*, **58** (2003) 172.

[25]. G. Zhou, P. R. Shah, T. K. P. Fornasiero, R. J. Gorte, "*Oxidation entropies and enthalpies of ceria–zirconia solid solutions*" *Catalysis Today* xxx (2007) xxx–xxx

[26]. C. Zhao,J. Vleugels, B. Basu and O. V. D. Biest, "*High toughness Ce-TZP by sintering in an inert atmosphere*", *Scripta Mater.*, **43** (2000) 1015.

[27]. B. D. Cullity, Elements of X-Ray Diffraction, Second Edition, 1978, p- 351.

[28]. A. T. Procopio, A. Zavaliangos and J. C. Cunningham, "*Analysis of the diametrical compression test and the applicability to plastically deforming materials*", J. Mat. Sc. **38** (2003) 3629.

[29]. W. E. Lee and W. M. Rainforth, "*Ceramic Microstructures: Property control by processing*", 1st edition, p-34, Chapman and Hall, 1994.

[30]. H. E Attaoui, M.Saadaoui, J. Chevalier and G.Fantozzi, "*Static and cyclic crack propagation in Ce-TZP ceramics with different amounts of transformation toughening*", *J. Euro. Ceram. Soc.*, **27** (2007) 483.

[31]. G. R. Anstis, P. Chantikul, B. R. Lawn, D. B. Marshall, "*A critical evaluation of indentation techniques for measuring fracture toughness: I. Direct crack measurements*", *J. Am. Ceram. Soc.*, **64** (1981) 533.

[32]. M. Matsui, T. Takashia and I. Oda, "*Effects of starting materials and calcining temperature on sintering of spinel ceramics. In Advances in Ceramics*", ed. W. D. Kingery, The Am. Ceram. Soc., Columbus, OH, **10**, (1984) 562.